SEMARAK ILMU PUBLISHING

Journal of Advanced Research in Fluid Mechanics and Thermal Sciences

Journal homepage:
https://semarakilmu.com.my/journals/index.php/fluid_mechanics_thermal_sciences/index
ISSN: 2289-7879

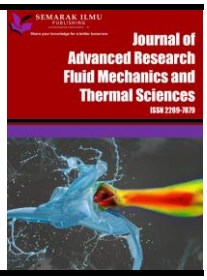

Impact of Non-Newtonian Fluids' Rheological Behavior on Double-Diffusive Natural Convection in an Inclined Square Porous Layer

Amina Ould Larbi[1], Redha Rebhi[2,3], Soufiane Rahal[4], Giulio Lorenzini[5,*], Laidi Maamar[1,4], Younes Menni[6], Hijaz Ahmad[7]

[1] Biomaterials and Transport Phenomena Laboratory (LBMPT), University of Medea, 26000 Medea, Algeria
[2] Department of Mechanical Engineering, Faculty of Technology, University of Medea, Medea 26000, Algeria
[3] LERM-Renewable Energy and Materials Laboratory, University of Medea, Medea 26000, Algeria
[4] Faculty of Technology, University Dr Yahia Fares of Medea, Medea, 26000 Medea, Algeria
[5] Department of Engineering and Architecture, University of Parma, Parco Area delle Scienze, 181/A, 43124 Parma, Italy
[6] Department of Technology, University Center Salhi Ahmed Naama (Ctr. Univ. Naama), P.O. Box 66, Naama 45000, Algeria
[7] Section of Mathematics, International Telematic University Uninettuno, Corso Vittorio Emanuele II, 39, 00186 Roma, Italy

ARTICLE INFO

Article history:
Received 10 April 2022
Received in revised form 4 August 2022
Accepted 15 August 2022
Available online 10 September 2022

Keywords:
Double-diffusive natural convection; Carreau-Yasuda model; buoyancy ratio; heat and mass transfer; non-Newtonian fluids

ABSTRACT

This paper presents a numerical study of double-diffusive convection in a square cavity with a porous layer filled with a non-Newtonian fluid and subjected to uniform Neumann heat and air flows applied to the active walls of the cavity, while the other walls are considered adiabatic and impermeable. We used the Carreau-Yasuda rheological model, which is adequate for many non-Newtonian fluids, and is used to characterize the behavior of the shear-tinning fluids. The finite difference method is used to obtain the numerical solution of the general governing equations, for a thin shear-thinning fluid with Darcy model and Boussinesq approximation were employed to model the convective flow in the porous medium. The governing parameters of the problem are the rheological parameters of Carreau-Yasuda, namely (n, E, s and a), the thermal Rayleigh number , R_T, the Lewis number Le, the buoyancy ratio N, and inclination angel, Φ. the effects of the mentioned governing parameters, flow intensity, apparent viscosity, and heat and mass transfer rates, were illustrated and discussed in terms of steamlines, isotherm, isoconcentration, apparent viscosity contours, stream function, apparent viscosity profiles, the average Nusselt number and the average Sherwood number. The results indicate a strong influence of the shear behavior of the non-Newtonian fluid on the heat and mass transfer by natural convection inside the enclosure. the flow structure evolves from conduction to convection as the buoyancy ratio increases. The Nusselt, Nu, and Sherwood, Sh, numbers increase along the transition path. The average number of Sh increases considerably with the improvement of the number of Lewis number but the average number of Nu changes slightly. The thermal and mass transfer is favored for an angle of inclination of 45°.

* *Corresponding author.*
E-mail address: lorenzini.unipr@gmail.com

https://doi.org/10.37934/arfmts.99.1.1747

1. Introduction

The study of thermosolutal convection in porous media is currently the subject of numerous works at the international level. It consists in studying the convective movements induced in a porous medium by a temperature gradient and a concentration gradient (caused by variation with temperature and/or solute concentration in the presence of a gravitational field). The movements generated by the variations of the density of the saturating fluid as a function of temperature and concentration can be very different from the classical case of natural convection of thermal origin [1]. The study of convection within enclosures filled with non-Newtonian fluids would help to improve the design and performance of a variety of engineering and environmental application processes such as thermal and chemical engineering, slurry transporting, food processing, migration of moisture in insulating fibers, crystal growth, petroleum drilling, hydrology, polymer engineering, geophysics, mixtures separation, gas storage, and in many other industrial processes, etc.

A rather complete review of these works has been made by number of publications [2-5]. Due to the conflicting volumetric forces of thermal and solutal forces, convection by double-diffusion is fundamentally defined by the phenomena of heat and mass transfer, which are the source of entropy creation, Wang *et al.,* [6]. In a porous medium, Chen and Chen [7] numerically studied the natural convection in a porous horizontal circular cylinder and a sphere filled with a non-Newtonian fluid, using a power-law model. They showed that the heat and mass characteristics for the natural convection of a non-Newtonian fluid with low power-law index values in the porous medium are worth studying. Yang and Wang [8] investigated the natural convection heat transfer of non-Newtonian fluids of power-law type with flow constraints. Mahrous *et al.,* [9] reviewed the different assumption used to calculate blood viscosity in CFD models of intracranial aneurysm.

Non-Newtonian fluids in porous media behave substantially differently from Newtonian fluids in porous media in terms of convective heat and mass transfer. Because non-Newtonian fluids are non-linear, their effects on porous media are distinct from those of Newtonian fluids. Pascal has thought about the flow of non-Newtonian fluids with a power-law through a porous medium, Pascal [10,11]. A modified version of Darcy's law that uses an extended Bingham rheological model to describe the flow through a simple capillary tube for non-Newtonian fluids. The first investigation of double-diffusive convection in a porous layer based on Darcy's law, which is applicable to dense, low-permeability porous media, was done by Taunton *et al.,* [12]. The commencement of motion was predicted using the linear permeability theory on a layered horizontal porous layer with a stable, inactive concentration that was heated and salted from the ground. A vertical plate in a saturated porous medium subjected to constant and uniform active wall temperature and concentration was examined by Jumah and Mujumdar [13] for heat and mass transfer by natural convection on non-Newtonian power-law fluids with flow constraint. Non-Newtonian liquids are characterized by shear-thickening and shear-thinning materials, which have different influences on heat transport operations. Thus, shedding light on the heat transport attributes of non-Newtonian liquids at different working stresses helps to increase their heat transport efficiency. Here, we used the tile model for the analysis of flow behavior in which viscosity depends on shear rate. Al-Azawy *et al.,* [14] numerically studied the three-dimensional, steady, laminar and non-Newtonian Carreau model blood flow through a stenosis artery. The shape of stenosis that has been selected is a trapezoidal with two cases (70% and 90% blockage). Shear-rate, streamlines, vorticity and importance factor were examined to assess the influence of non-Newtonian model. They showed that the levels of non-Newtonian model were predicted to be higher in the 90% blockage then that observed within the 70%. An examination of streamlines through the artery advised that the recirculation areas in the artery and after the stenosis stretched further in the Carreau model. Unuh *et al.,* [15] carried out a

numerical study of magnetic flux and shear-stress of OEM damper featuring MR fluid. The finite element model was built to analyse and examine the new design of OEM damper. Their main finding was that the induced magnetic field can manifest the shear stress development by polarizing the suspended partial in the MR fluid. In addition, the gradient of shear stress response decreased at highest shear stress and eventually become plateaus as the MR fluids saturated completely.

Wang *et al.,* [16] investigated the natural convection of a non-Newtonian power-law fluid in a square porous cavity. The authors have solved the problem analytically and numerically using the fourth-order Runge-Kutta scheme and the shooting method. From the reported numerical results, it was found that the onset of natural convection would occur if a minimum value for the yield stress is provided. Jecl and Škerget [17] applied the boundary finite element method to study the natural convection in non-Newtonian fluid in a square porous cavity. Power-law and Carreau model are used to model non-Newtonian rheological behavior. The results of the hydrodynamic and heat transfer evaluations were reported for the configuration in which the enclosure is heated by a side wall while the horizontal walls are insulated. The flow in the porous medium a was modeled using the modified Brinkman extended Darcy model, taking into account non-Darcy viscous effects. Lamsaadi *et al.,* [18] studied the effect of power index on natural convection in the rectangular cavity with constant heat flow on the side walls and adiabatic vertical walls for the high Prandtl number limit. Compared to Newtonian fluids (*n*=1), a decrease in the power-law index n (shear-thinning fluids, 0 < n < 1Þ) induces an early onset of the single-cell flow regime and increases the convective heat transfer rate, whereas an increase in *n* (shear-thickening fluids, *n* > 1) produces an opposite effect. Contrary. The main results of the approximate solution of the parallel flow have been validated numerically. Natural convection in a rectangular porous medium is studied analytically and numerically by Bahloul [19]. He showed that the thermal stratification coefficient, depends essentially on the aspect ratio of the enclosure and that it becomes almost independent of the Rayleigh number in the boundary layer regime. For high heating, he gave a simplified model for the stratification parameter $\gamma = 1.22A^{-0.47}\ Ra^{0.46}$. The linear stability study of the parallel flow has been used to determine the critical Rayleigh number for a cavity of large extension. The author found that the flow is stable regardless of the stratification coefficient. The natural convection flow, heat and mass transfer of non-Newtonian power law fluids with flow constraint in a porous medium from a vertical plate with varying heat and wall mass fluxes were considered by Cheng [20], he observed that the existence of a threshold pressure gradient in power law fluids tends to decrease the fluid velocity and the local Nusselt and Sherwood numbers. Similarly, an increase in the power law exponent increases the local Nusselt and Sherwood numbers.

The natural convection of non-Newtonian power-law fluids in a porous cavity was numerically studied and described by Hadim [21] using the modified Brinkman-Forchheimer model. He concluded that as the power-law index decreases, the circulation inside the enclosure increases, leading to a higher Nusselt number. These effects are enhanced as the Darcy number increases. This results in a higher vertical velocity near the walls and a higher Nusselt number in the cavity. Therefore, an increase in the Rayleigh number produced similar effects to a decrease in the power-law index. Cheng's [20] research on the Nusselt and Sherwood numbers shows that they rise as the power-law increases. A mathematical analysis of thermosolutal convection in a porous media was published by Lin and Payne [22]. This study employed the Darcy model. The flow solution is continuously dependent on the Soret effect, according to the authors. Current findings on asymptotic and numerical double-diffusion convection in the presence of a magnetic field was conducted by Rebhi *et al.,* [23,24]. Neumann and Dirichlet boundary conditions for temperature and solute concentrations were used to generalize the study. various convection mechanisms, and solute concentrations, were noted.

The topic of coupled, stable, laminar heat and mass transmission through a permeable wedge immersed in a porous medium with variable surface temperature and concentration, as well as heat generation or absorption and wall transpiration effects, was examined by Chamkha [25]. In the presence of Soret and Dufour parameters, Kefayati [26,27] examined the naturally occurring double-diffusive convection of non-Newtonian power-law fluids and entropy generation in an inclined porous cavity. The impact of Carreau-Yasuda rheological parameters on natural convection in a horizontal porous cavity saturated with a non-Newtonian fluid was examined analytically and numerically by Khechiba *et al.,* [28]. The parallel flow assumption was used to generate the analytical solution. Zhu *et al.,* [29] investigated a numerical study of 3D double-diffusive natural convection in a fluid-saturated porous cubic enclosure by a generalized non-Darcy model. Wahid *et al.,* [30] carried out an analytical study the magnetohydrodynamic slip Darcy flow of viscoelastic fluid over stretching sheet and heat transfer with thermal radiation and viscous dissipation. Their main conclusions that the elastico-viscous fluid ($k_1^* < 0$) enhances the skin friction coefficient and reduce the heat transfer coefficient compared to second grade fluid. Parvin *et al.,* [31] investigated the magnetohydrodynamics Casson fluid flow, heat mass transfer due to the presence of assisting flow and Buoyancy ratio parameters. They showed that the increment and decrement of the velocity, temperature, concentration, skin friction coefficient, local Nusselt number and local Sherwood number are influenced by magnetic field, assisting flow and buoyancy ratio parameters.

Recently, using the Dupuit-Darcy model, Rebhi *et al.,* [32,33] conducted analytical and numerical studies of convective fluxes created in vertical and horizontal porous cavities filled with a binary mixture. studying the linear stability of the parallel flow approximation, the authors explicitly and implicitly predicted the onset of convective motion and the trigger point of the Hopf bifurcation characterizing the transition between stable convective and oscillatory states. They showed a considerable impact of the shape drag on the critical conditions and the heat and mass exchange rates. Multiple stable and oscillatory solutions coexisted near the criticality and vertically moving waves were observed. The linear and double-diffusive convection in a horizontal porous medium filled with a linked nano-fluid was analytically and numerically explored by Khan *et al.,* [34]. The Fourier series method employed the equation regulating the phenomenon. The Dufour effect and the Soret effect are two examples of concentration gradient-induced heat flow and temperature gradient-induced material flow, respectively. They discovered that the torque constancy parameter enhances the system's stability in both oscillatory and stationary convection modes. A theoretical and numerical study of Soret-induced convection in a horizontal porous layer saturated with a mixture of n components was conducted by Mutschler and Mojtabi [35]. Ali *et al.,* [36]. studied the impact of magnetic field on the flow behavior of a non-Newtonian Casson fluid in a constricted channel using Darcy's law for steady and pulsatile flows. The wall shear stress (WSS) had an incentive trend as a function of the magnetic parameter, Strouhal number, and Casson parameter. In addition, the flow separation region can be controlled by the magnetic parameter. Analytical and numerical solutions of 2D sakiadis flow of non-Newtonian Casson fluid with convective boundary conditions based on the Buongiorn's mathematical model was studied by Ghiasi and Saleh [37]. They found that the skin friction coefficient for non-Newtonian fluid is found to be higher than that of the Newtonian one. In addition, the thermal boundary layer thickness is greatly affected by the resistive Lorentz force and viscous dissipation. Wang *et al.,* [38] studied numerically the implications of temperature-dependent viscosity and thermal conductivity for heat and mass transport of Williamson nanofluids across a nonlinear stretching sheet of irregular thickness are examined when biconvection of microorganisms is incorporated. They found that the value of Brownian motion and Lewis number reduce the concentration of nanoparticles. In addition, the velocity of non-Newtonian is less than the viscous nanofluid but temperature behaves oppositely. Khdher *et al.,* [39] studied the secondary flow

configuration in square straight channel with heat transfer enhancement of water and three different types nanofluids (Al_2O_3, TiO_2 and CuO) water a base fluid under constant heat flux in upper and lower walls. CFD software were employed to perform the investigation numerically in the range of Reynolds number 104-106. They concluded that by increasing Reynolds number the secondary flow increases as well as shear stress is increase. In addition, the volume concentration increases, the wall shear stress and heat transfer rates increase. Nanofluid with CuO, nanoparticle achieved higher Nusselt number followed by TiO_2 and Al_2O_3, respectively. The steady of stagnation point flow and radiative heat transfer of a non-Newtonian fluid which is Casson fluid passing over an exponentially permeable slippery Riga plate was studied by Yusof *et al.,* [40]. They recorded that the momentum boundary layer thickness increases with increasing the values of Casson parameter. The temperature decreases when the velocity slip parameter and thermal slip parameter are increased. Khan *et al.,* [41] studied the effectiveness of utilizing the suspension of nanoparticles in water at supercritical pressures in the mitigation of heat transfer deterioration. The thermohydraulic performances of the supercritical water-based nanofluids are analysed using the dimension less parameters based on normalized Nusselt numbers and Fanning friction factors. They concluded that the increasing nanoparticles delayed and weekend the HTD at pseudocritical region. In addition, increasing nanoparticles increase the overall thermal performance of the base fluid. Significance of biconvection and mass transpiration for MHD micropolar Maxwell nanofluid flow over an extending sheet, was studied by Habib *et al.,* [42]. The similarity variable was used to transform the flow equations into corresponding non-dimensional ODEs. It was reported that motile density profile is decline when Lewis and Peclet numbers are boosted. In addition, the temperature distribution increased for large values of Brownian motion, Rayleigh number and thermophoresis parameters. Awan *et al.,* [43] published a comparative study of hybrid nano liquid (Al_2O_3, Cu/Water) and nano liquid (Al_2O_3/water) over the linearly extending surface. They found out that the Al_2O_3-Cu nano particles proved to be a better heat transforms as compared to Al_2O_3 nano particle.

In shallow and finite aspect ratio enclosures, Rebhi *et al.,* [44] investigated numerically and analytically the influence of the rheological behavior of non-Newtonian fluids on Rayleigh-Bénard thermosolutal convection instabilities. In an inclined square hollow filled with a non-Newtonian liquid subjected to uniform and constant concentrations and temperatures, while the outer walls are impermeable and adiabatic. The Carreau-Yasuda model was used to represent the rheological behavior of non-Newtonian fluids. These authors studied the effect of the rheological parameters of the model used on the bistability of thermosolutal convection. Lounis *et al.,* [45] statistically explored thermosolutal convection with Soret and Dufour effects. For various values of the governing parameters, the results were presented and examined in terms of streamlines, isotherms, iso-concentration, stream function, and average Nusselt and Sherwood numbers. For increasing Soret and Dufour parameters, heat exchange increases.

This paper studies heat and mass transfer by natural convection inside a saturated square cavity in a porous medium filled with a non-Newtonian fluid. The Carreau-Yasuda model is adopted to represent the behavior of non-Newtonian fluids. The active cavity walls are subject to either Neumann-type thermal and solutale boundary conditions (constant heat and concentration fluxes). The numerical method used to solve the set of governing equations uses the time-accurate finite difference method. The effect of different control parameters, namely, thermal Rayleigh number R_T, buoyancy ratio, N, Lewis number, Le, cavity tilt angle, Φ, and different C-Y parameters (n, E, a and s). The results are discussed in terms of flow function, apparent viscosity, and iso-thermal and iso-concentration lines. Variation of apparent viscosity, flow function, temperature and concentration and profiles, and heat and mass transfer rate.

2. Physical and Mathematical Model

The physical model described in Figure 1 considers a double-diffusive convection in a square porous cavity filled with a non-Newtonian fluid. The axes of coordinates *x, y* are respectively oriented according to the horizontal and vertical directions. The active walls of this cavity are subjected to a uniform density of heat and mass fluxes while the others are assumed to be adiabatic and impermeable. The rheological behavior of a non-Newtonian fluid can be described by the Carreau-Yasuda model [44-48].

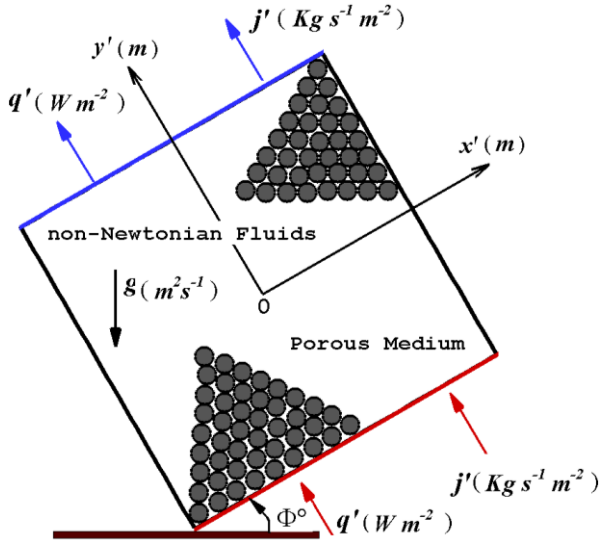

Fig. 1. Schematic of the physical model

The fluid is assumed to be a laminar, incompressible, non-Newtonian, low shear flow. the thermophysical properties are constant, except for the effect of density variation in the buoyancy term. Using the Boussinesq approximation, the variation of the density with temperature and concentration is described by the linearized equation of state as [49]

$$\rho = \rho_0 \left[1 - \beta_T \left(T' - T_0' \right) - \beta_s \left(C' - C_0' \right) \right] \tag{1}$$

where ρ is the fluid density ρ_0 is s the medium density at the Reference at temperature *T* and concentration *C* which represents the temperature and concentration values at the origin of the coordinate system, and β_T and β_s are the thermal expansion coefficient and the concentration coefficient, respectively which are defined by $\beta_T = -\frac{1}{\rho_0}\left[\frac{\partial \rho}{\partial T'}\right]_C$ and $\beta_C = -\frac{1}{\rho_0}\left[\frac{\partial \rho}{\partial C'}\right]_T$.

The governing equations that describe the thermal behavior of the system are conservation of momentum, energy and solute balances by [28]

$$\nabla^2 \psi' = -\frac{gK\beta_T}{\nu}\left[\frac{\partial}{\partial x}\left(T' + \frac{\beta_s}{\beta_T}C'\right)\cos\Phi + \frac{\partial}{\partial y}\left(T' + \frac{\beta_s}{\beta_T}C'\right)\sin\Phi\right] \tag{2}$$

$$(\rho C)_P \frac{\partial T'}{\partial t'} + (\rho C)_\rho V'.\nabla T' = k\nabla^2 T' \tag{3}$$

$$\varphi \frac{\partial C'}{\partial t'} + V'.\nabla C' = D\nabla^2 C' \tag{4}$$

where $(\rho C)_p$ and $(\rho C)_f$ are respectively the heat capacity of the saturated porous medium and the fluid, V' is the Darcy speed, g is the gravitational acceleration, *v* is the kinematical viscosity, *k* and *D* are the heat conductivity and the isothermal diffusion coefficient, ϕ is the normalized porosity of the porous medium, ψ', the stream function is defined such that $v' = -\partial\psi'/\partial x'$, $u' = \partial\psi'/\partial y'$.

In the present work, the fluid considered is a purely viscous fluid, it is a rheofluidic fluid whose viscosity, μ, obeys the Carreau-Yasuda model [44-48]

$$\frac{\mu - \mu_\infty}{\mu_0 - \mu_\infty} = \left[1 + \left(E'\dot{\gamma}'\right)^a\right]^{(n-1)/a} \tag{5}$$

where μ_0 represents is the fluid's viscosity at zero shear rates, μ_∞ is the fluid's viscosity at infinite shear rates. The shear-thinning index is shown by $n < 1$. The fluid's time character is represented by E'. $\dot{\gamma}'$ is the shear rate amplitude, and the transition between the zero-shear-rate zone and the power-law area is described by the dimensionless parameter a.

In order to proceed to the numerical solution of the system, we introduce the following non-dimensional variables [26,27]

$$(u, y) = \frac{(x', y')}{H'},\ t = \frac{t'\alpha}{\sigma H'^2},\ (u, y) = \frac{(u', v')H'}{\alpha},\ \psi = \frac{\psi'}{\alpha},\ \varepsilon = \phi/\sigma,\ T = \frac{(T' - T_0')}{\Delta T^*},\ C = \frac{(C' - C_0')}{\Delta C^*},$$
$$\Delta T^* = \frac{q'H'}{k},\ \Delta C^* = \frac{j'H'}{\rho_0 D},\ \mu_{CY} = \frac{\mu}{\mu_0},\ E = \frac{E'\alpha}{\varepsilon H'^2} \tag{6}$$

where k and α are the thermal conductivity and thermal diffusivity respectively and μ_0 is the dynamic viscosity of a Newtonian fluid.

The mass, momentum, energy, and concentration equations, considering the applied assumptions are as

$$\frac{\partial}{\partial x}\left(\mu\frac{\partial\psi}{\partial x}\right) + \frac{\partial}{\partial y}\left(\mu\frac{\partial\psi}{\partial y}\right) = -R_T\left[\frac{\partial}{\partial x}(T + NC)\cos\Phi + \frac{\partial}{\partial y}(T + NC)\sin\Phi\right] \tag{7}$$

$$\frac{\partial T}{\partial t} + \frac{\partial\psi}{\partial y}\frac{\partial T}{\partial x} - \frac{\partial T}{\partial y} = \nabla^2 T \tag{8}$$

$$\frac{\partial C}{\partial t} + \frac{\partial\psi}{\partial y}\frac{\partial C}{\partial x} - \frac{\partial\psi}{\partial x}\frac{\partial C}{\partial y} = Le^{-1}\nabla^2 C \tag{9}$$

In this study, the behavior of the non-Newtonian fluid is described by the non-Newtonian is described by the phenomenological constitutive model of Carreau-Yasuda [44-48].

$$\mu_{CY}(\gamma)=\mu(\gamma)=s+(1-s)\left[1+\left(E|\dot{\gamma}|\right)^{a}\right]^{(n-1)/a} \tag{10}$$

where μ denotes the apparent viscosity that is shear-dependent is the dimensionless shear-dependent apparent viscosity. $s=\mu_{\infty}/\mu_{0}$, is the report of viscosities with infinite to zero shear-rates. E a dimensionless time constant, whose inverse is the critical shear rate marking the beginning of shear-thinning. a is dimensionless parameter describing the transition region between the zero shear-rate region. n , which is less than unity for pseudoplastic fluids, is the exponent of the power-law that characterizes the shear-thinning regime. The following is how the dimensionless rate-of-strain $\dot{\gamma}$ is expressed

$$\dot{\gamma}=\left[4\left(\frac{\partial^{2}\psi}{\partial x\partial y}\right)^{2}+\left(\frac{\partial^{2}\psi}{\partial y^{2}}-\frac{\partial^{2}\psi}{\partial x^{2}}\right)^{2}\right]^{1/2} \tag{11}$$

The system's walls are subjected to the equivalent dimensionless boundary conditions, which are [28]

$$u=v=0,\ \psi=0,\ \frac{\partial\psi}{\partial x}=\frac{\partial\psi}{\partial y}=0 \tag{12}$$

and the thermal and solutal boundary conditions

$$\frac{\partial T}{\partial x}=\frac{\partial C}{\partial x}=0 \text{ at } x=\pm\frac{1}{2}, \text{ and } \frac{\partial T}{\partial y}=\frac{\partial C}{\partial y}=-1 \text{ at } y=\pm\frac{1}{2} \tag{13}$$

The fluid flow, heat and mass transfer are characterized by the following parameters dimensionless parameters, namely the Darcy-Rayleigh number, R_{T} , the buoyancy ratio, N , the Lewis number, Le , and the normalized porosity, ε .

$$R_{T}=\frac{\rho_{0}\beta\Delta T'KH'}{\mu_{0}\alpha},\ N=\frac{\beta_{s}\Delta C^{*}}{\beta_{T}\Delta T^{*}},\ Le=\frac{\alpha}{D},\ \varepsilon=\frac{\phi}{\sigma} \tag{14}$$

The local and average Heat and mass transfer rates on the hot wall can be expressed in terms of the Nusselt and Sherwood numbers and can be obtained from the following expressions

$$Nu^{-1}=\Delta T=T_{(0,-1/2)}-T_{(0.1/2)} \text{ (Neumann) or} \tag{15}$$

$$Nu=-\left.\frac{\partial T}{\partial y}\right|_{y=\pm 1/2} \text{ (Dirichet) and} \tag{16}$$

$$Nu_{m}=A^{-1}\int_{-A/2}^{A/2}Nu\,dx \tag{17}$$

$$Sh^{-1} = \Delta C = C_{(0,-1/2)} - C_{(0.1/2)} \text{ (Neumann) or} \tag{18}$$

$$Sh = -\left.\frac{\partial C}{\partial y}\right|_{y=\pm 1/2} \text{ (Dirichet) and} \tag{19}$$

$$Sh_m = A^{-1} \int_{-A/2}^{A/2} Sh dx \tag{20}$$

3. Numerical Solution

Previously discretized using the conventional centered approach. For convective flow simulations in a two-dimensional porous layer saturated with a non-Newtonian fluid, a double precision FORTRAN-95 algorithm was created.

First, the time terms that appeared in the governing equations based on the implicit alternating direction technique were discretized for the two-dimensional governing Eq. (7) to Eq. (9) using a second-order backward finite difference scheme (ADI).

To accelerate the convergence of the program and avoid the divergence of the solution at each time step, we used the sub-relaxation technique. The following convergence condition has been verified

$$\frac{\sum i \sum j \left|\psi_{i,j}^{k+1} - \psi_{i,j}^{k}\right|}{\sum i \sum j \left|\psi_{i,j}^{k}\right|} \leq 10^{-8} \tag{21}$$

where $\psi_{i,j}$ is the value of the stream function at the iteration's node (i, j).

For thermosolutal natural convection, the best numerical results were achieved in a square cavity with a non-Newtonian fluid inside of it. For the Neumann and Dirichlet thermal boundary conditions, respectively, the results of the current technique were compared with those given by numerous publications as shown in Table 1 to Table 3. It was discovered that the uniform mesh size of ($N_x \times N_y = 100 \times 100$) provided good agreement between the current results and the information published in prior investigations.

Table 1
Comparison of ψ_0, Nu, Nu_m, and μ with some previous studies numerical results for Neumann thermal boundary conditions, $R_T = 50$, $E = 0.2$, $s = 10^{-2}$, $a = 2$ and versus n

Neumann thermal boundary conditions									
n	Khechiba *et al.,* [28]			Present study			Present study vs Khechiba *et al.,* [28]		
	1	0.8	0.6	1	0.8	0.6	1	0.8	0.6
ψ_0	1.915	2.235	2.872	1.914	2.235	2.869	0.05(%)	0.00(%)	0.10(%)
Nu	1.912	2.221	2.778	1.912	2.221	2.777	0.00	0.00	0.03
Nu_m	1.719	1.964	2.431	1.719	1.964	2.431	0.00	0.00	0.00
μ	…	…	…	1.000	0.815	.456	…	…	…

Table 2
Comparison of ψ_0, Nu, Nu_m, and μ with some previous studies numerical results for Dirichlet thermal boundary conditions, $R_T = 70$, $E = 0.6$, $s = 10^{-2}$, $a = 2$ and versus n

Dirichlet thermal boundary conditions									
n	Khechiba *et al.,* [28]			Present study			Present study vs Khechiba *et al.,* [28]		
	1	0.8	0.6	1	0.8	0.6	1	0.8	0.6
ψ_0	3.715	6.685	14.017	3.717	6.716	14.076	2.74(%)	0.46(%)	0.42(%)
Nu	2.139	3.253	4.707	2.139	3.261	4.717	0.00	0.24	0.21
Nu_m	2.046	3.178	5.148	2.046	3.185	5.148	0.00	0.22	0.00
μ	…	…	…	1.000	0.525	0.169	…	…	…

Table 3
Validation of the numerical code in terms of the flow function at the center of the cavity, ψ_{max}, the Nusselt number, Nu_m, and the Sherwood number, Sh_m for $R_T = 100$, $N = -0.8$, $Le = 10$ and $A = 4$

	Benhadji [50]	Mamou and Vasseur [51]	Present study	Present study vs Benhadj [50]	Present study vs Mamou and Vasseur [51]
ψ_{max}	3.695	3.689	3.688	0.18(%)	0.02(%)
Nu_m	3.653	3.635	3.643	0.27	0.21
Sh_m	6.747	6.737	6.743	0.05	0.08

4. Results and Discussion

The results are performed for different quantities of the Carreau-Yasuda parameters, i.e., n, E, s, and a, thermal Rayleigh number, R_T, buoyancy ratio, N, Lewis number, Le, and inclined angel, γ. Numerical results are provided in the range of: $0.4 \le n \le 1$, $0 \le E \le 0.6$, $0 \le s \le 1$, $0.85 \le a \le 2$, $0 \le R_T \le 100$, $10^{-1} \le Le \le 10^2$, $-5 \le N \le 5$ and $0° \le \Phi \le 90°$. Figure 2 shows the effect of power law index, n, on the streamlines, isotherms, iso-concentrations, and the contours of the apparent viscosity of the square cavity, are presented from left to right, respectively. It can be seen clearly with a decrease in the power-law index, n, the streamlines become elliptical in the center of the cavity, the convection improves. Also, increases both the thermal amplitudes and the concentration of is on the hot wall. This confirms that decreasing of the power-law index, n, enhances heat transfer and mass. The apparent viscosity also changes with the change in power index, n, the transition from a Newtonian fluid ($n = 1$) to a non-Newtonian fluid ($n < 1$) is more complex and distorted.

Figure 3 presents the different time constant parameter, E, on the streamlines, isotherms, iso-concentrations and apparent viscosity contours for the square cavity. Increasing the, E , parameter increases the expansion of loops. Furthermore, the iso-concentrations gradient on the thermal wall decreases by the parameter, E, decreases from 0 to 0.6. the mass transfer improves when e decreases. Also, if the amount of parameter, E, is reduced, the fluid becomes highly viscous (when E =0 → Newtonian fluid μ=1).

Figure 4 displays streamlines, isotherms, iso-concentrations, and apparent viscosity in different values of values of the ratio of infinite to zero shear rate viscosities, s. The movement of the streamlines is confirmed by the decrease of parameter, s. Also, the contours show that the iso-concentrations density on the hot wall increases with decreasing parameter, s. On one hand, the apparent viscosity of the fluids is improved (Newtonian fluid).

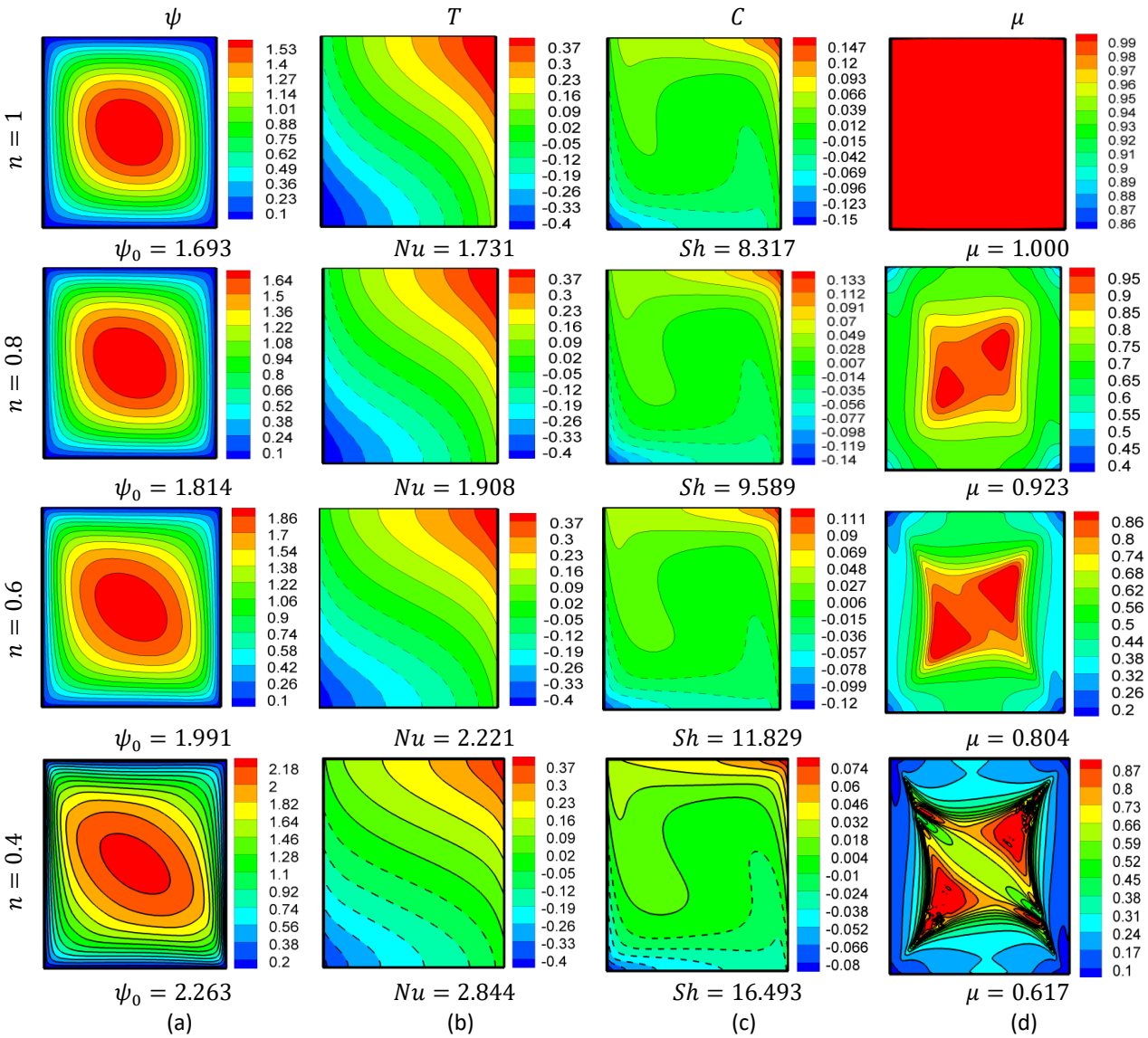

Fig. 2. Effect of the power-law index, n, on : (a) streamlines, (b) isotherms, (c) is-concentrations and (d) apparent viscosity contours for R_T = 50, E = 0.2, S = 0.01, a = 2, Le =10, N =-0.5 and Φ=0°

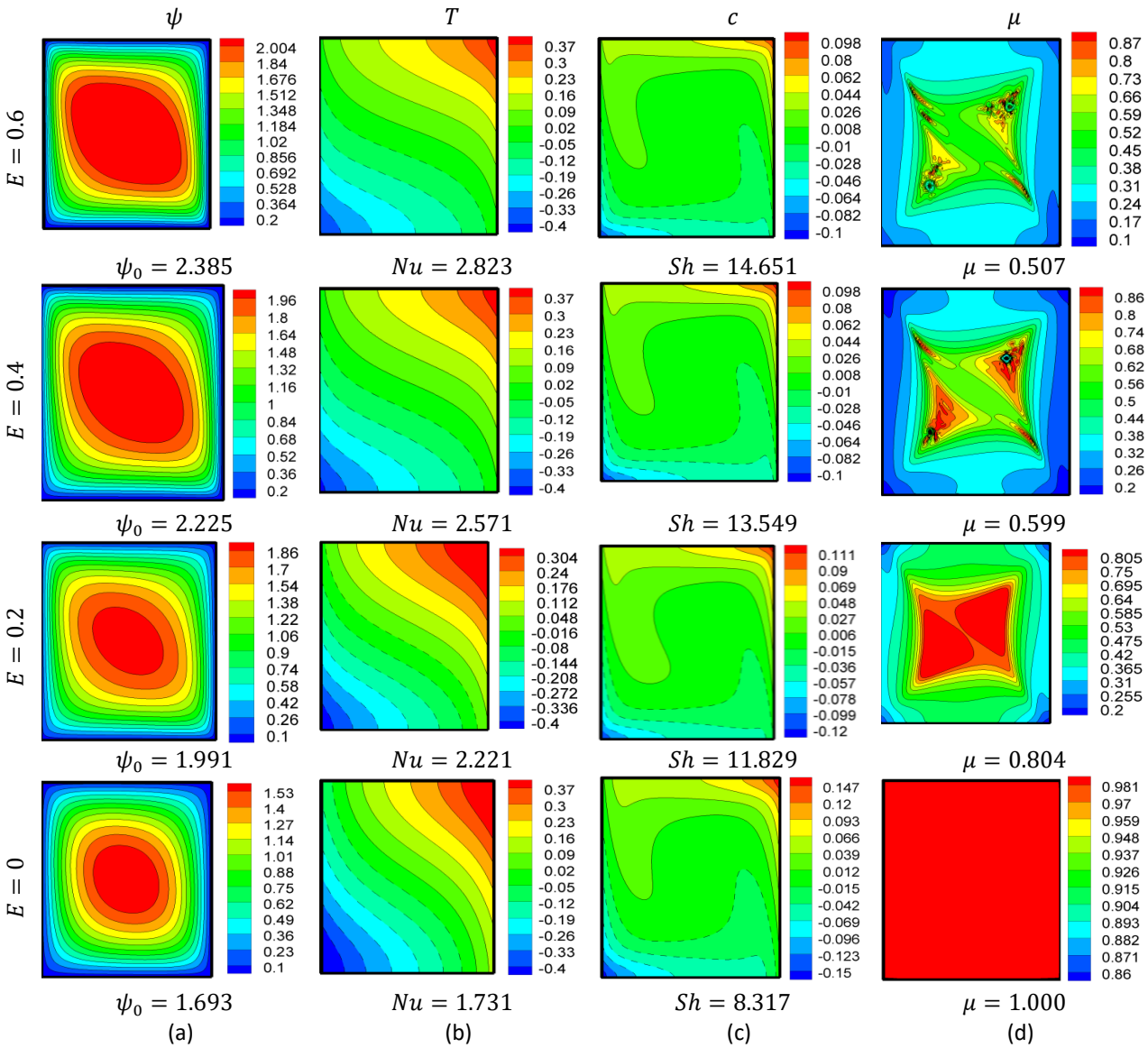

Fig. 3. Effect of the Time constant number, E, on : (a) streamlines, (b) isotherms, (c) is-concentrations and (d) apparent viscosity contours for R_T = 50, S = 0.01, n = 0.6, a = 2, Le =10 , N =-0.5 and Φ=0°

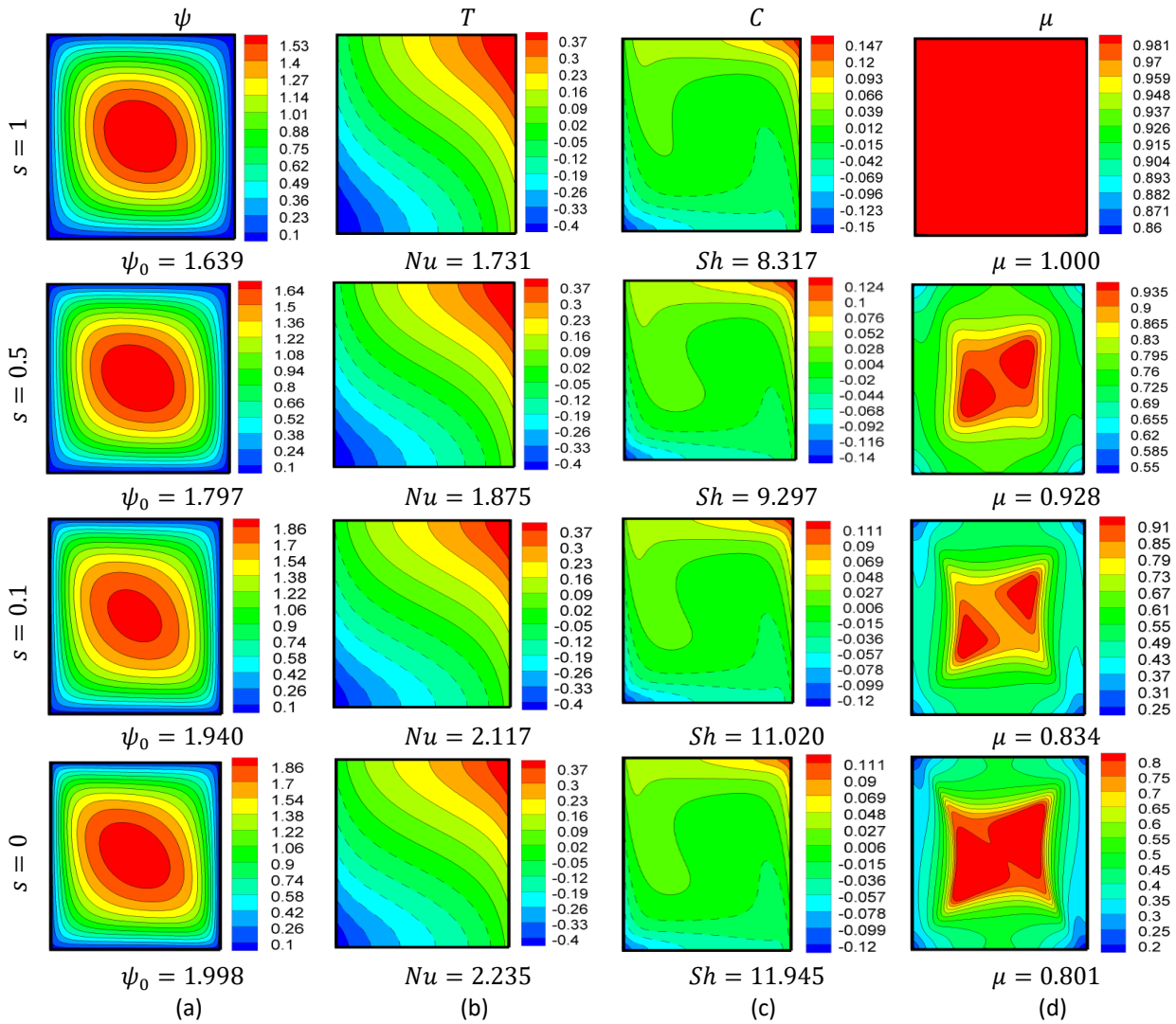

Fig. 4. Impact of the different parameter, s, on : (a) streamlines, (b) isotherms, (c) is-concentrations and (d) apparent viscosity contours for R_T = 50, E = 0.2, n = 0.6, a = 2, Le =10, N =-0.5 and Φ=0°

Figure 5 resumes different values of parameter, a. on the streamlines, isotherms, iso-concentrations, and the apparent viscosity. Comparing the flow models, a decrease in the parameter a increases the convection process. On one hand, when the parameter, a, decreases, the concentration density on the hot wall increases. similar to the temperature is improved by decrease the value of parameter, a. The pattern demonstrates that the process creates a rise in the gradient of temperature and concentration on the hot wall, which leads to an increase in heat and mass transfer as the parameter a are lowered. In addition, the apparent viscosity increases with decrease of the parameter of, a, (a <1, shear-thinning fluids).

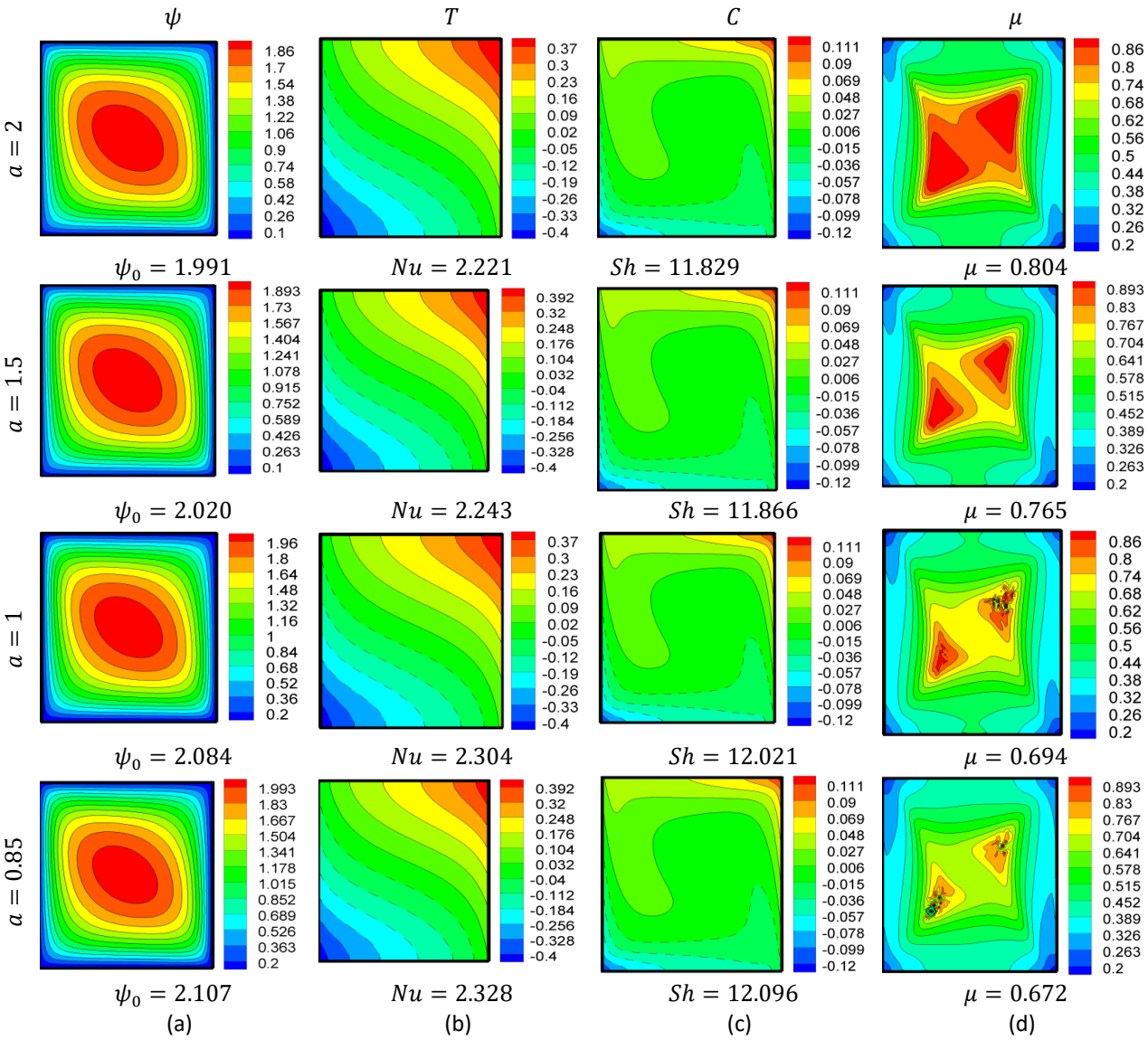

Fig. 5. Effect of the different parameter, a, on: (a) streamlines, (b) isotherms, (c) is-concentrations and (d) apparent viscosity contours for R_T = 50, $n = 0.6$, $E = 0.2$, $s = 0.01$, $Le = 10$, $N = -0.5$ and Φ=0°

Figure 6 shows how the stream-function, apparent viscosity, temperature, and concentration profiles are affected by the power-law index, n. The profiles are symmetrical with respect to the center of the cavity. Figure 6(a) shows that the flow function goes from zero at the walls to a maximum at the center of the system. Furthermore, the flow function increases with decreasing power-law index, n. the effect of the power index, n. while the fluid becomes thinner at shear. On the apparent viscosity μ as shown in Figure 6(b), increasing the power index, n, leads to an increase in the value of the viscosity to become constant (at Newtonian fluid). the effect of the power index, n, on the temperature profiles is shown in Figure 6(c) as the power index, n, decreases, the temperature decreases toward the center of the system. which leads to a significant increase in the convective heat transfer rate (i.e., Nu number). The concentration decreases with decreasing n and then increases towards the center of the cavity, as shown in Figure 6(d).

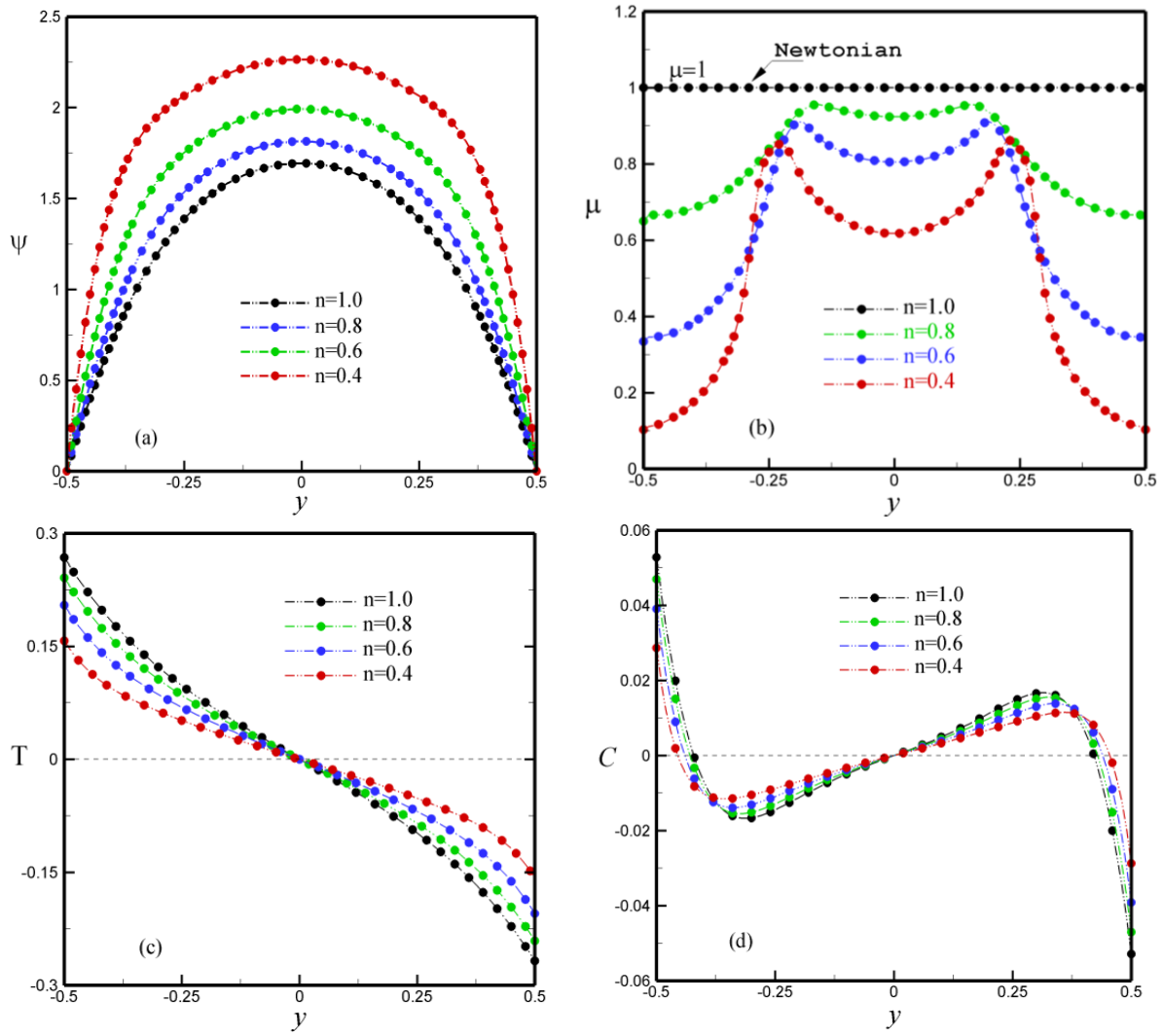

Fig. 6. Effect of the power-law index, n, on: (a) stream-function, ψ (b) apparent viscosity, μ, (c) temperature, T, and (d) concentration, C, profiles for $R_T = 50$, $E = 0.2$, $a = 2$, $s = 0.01$, $Le = 10$, $N = -0.5$ and Φ=0°

Figure 7 present of the different time constant parameter, E, on the stream-function, apparent viscosity, temperature and the concentration profiles. Figure 7(a) illustrates the flux intensity increase for large values of parameter, E. The apparent viscosity, μ, is symmetric about the center of the cavity, as shown in Figure 7(b). A decrease in the values of, E, results in an increase in the apparent viscosity from $E = 0.6$ (non-Newtonian fluid) to $E = 0$ (Newtonian fluid), so that the strength of convective motion is significantly increased by the increase in the value of E. Figure 7(c) and Figure 7(d) show that a decrease in the values of, E, results in a slight increase in the temperature and concentration difference between the walls.

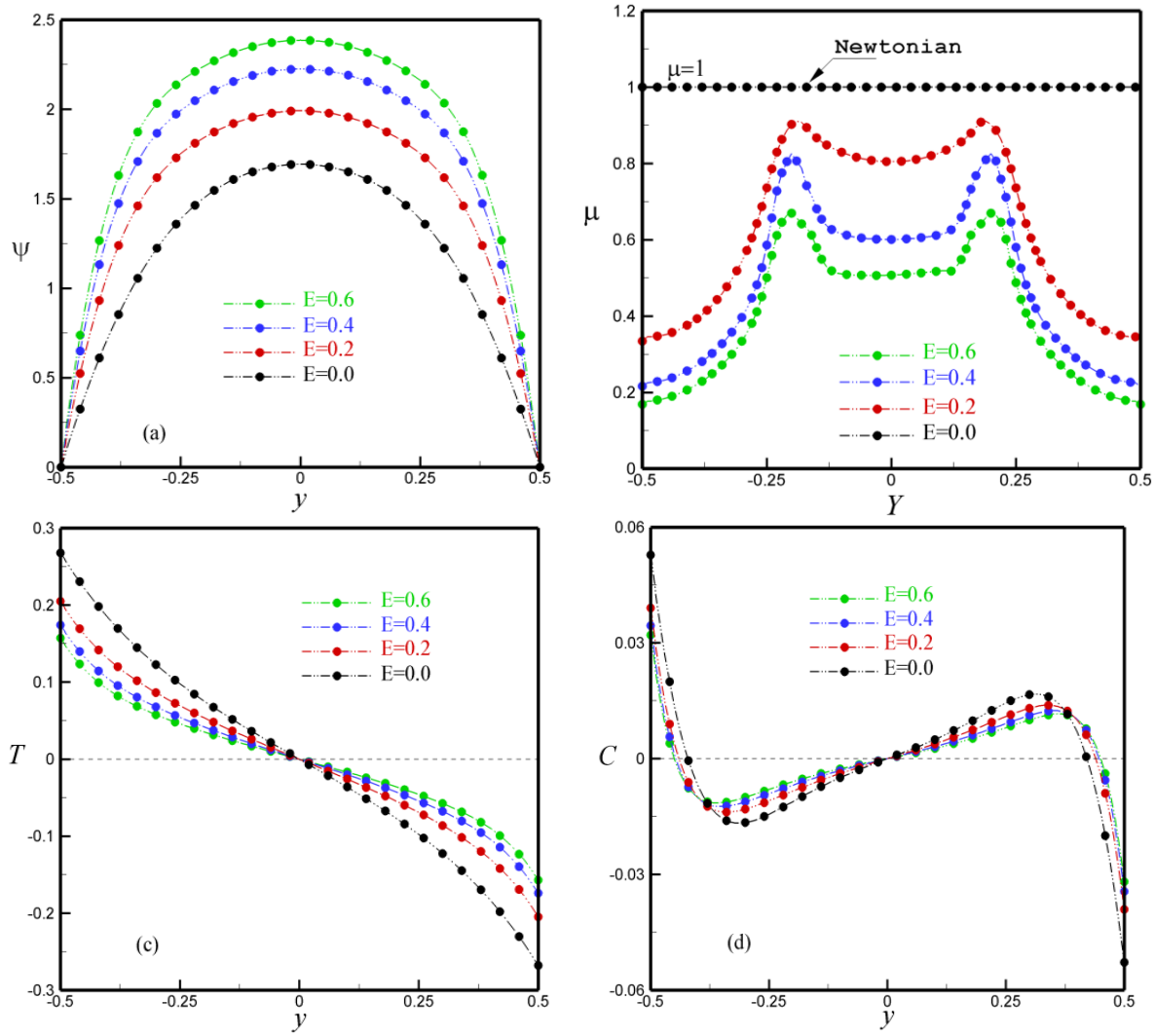

Fig. 7. Influence of the different time constant parameter, E, on: (a) stream-function, ψ (b) apparent viscosity, μ, (c) temperature, T, and (d) concentration, C, profiles for $R_T = 50$, $n = 0.6$, $a = 2$, $s = 0.01$, $Le = 10$, $N = -0.5$ and Φ=0°

The effects of the ratio of infinite to zero shear rate viscosities, s, on the temperature, concentration profiles, apparent viscosity, and stream function are shown in Figure 8. Figure 8(a) shows that a decrease in the parameter, s, leads to an increase in the flow intensity near the walls. The effect of parameter, s, on apparent viscosity, as shown in Figure 8(b), the shear- thinning effect becomes significant on the walls and center of the cavity as the parameter s decreases, resulting in a decrease in the viscosity of the fluid ($s = 1, \mu = 1$). The influence of the parameter, s, on the temperature profiles is shown in Figure 8(c). The temperature difference decreases with decreasing values of s from ($s = 1$ to $s = 0$). In addition, the strength of heat transfer by convection is moderately enhanced by decreasing this parameter, s. Figure 7(d) shows that the effect of the values of, s, results in a slight increase with the variation of the parameter, s.

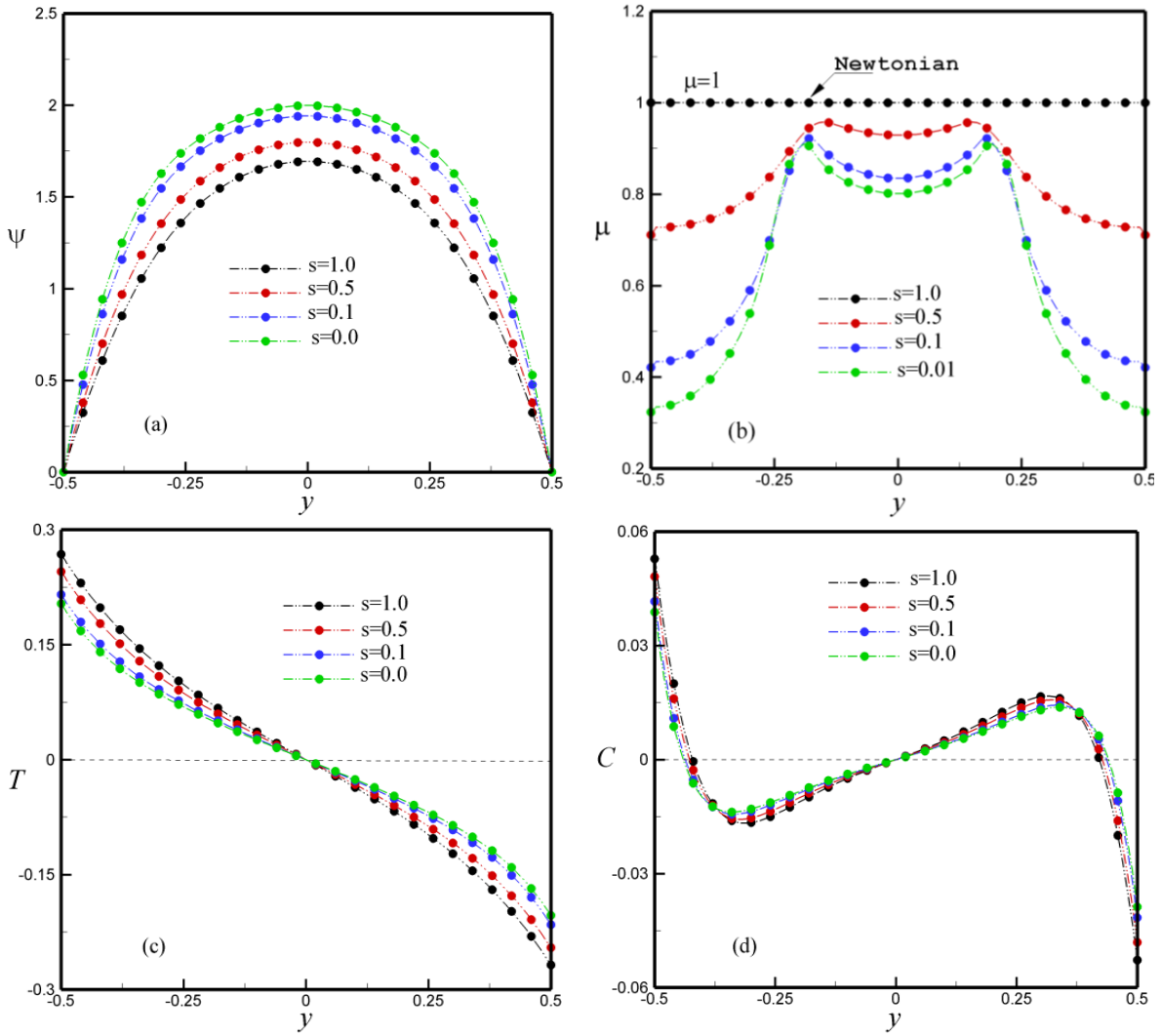

Fig. 8. Impact of the ratio of infinite-to zero-shear-rate viscosities, S, on (a) stream-function, ψ, (b) apparent viscosity, μ, (c) temperature, T, and (d) concentration, C, profiles for $R_T = 50$, $n = 0.6$, $a = 2$, $E = 0.2$, $Le = 10$, $N = -0.5$ and Φ=0°

Figure 9 displays the effects of parameter, a, on the stream-function, apparent viscosity, temperature and the concentration. Figure 9(a) shows the influence of the parameter, a, on the profiles of the flow function, it was observed that when the parameter, a, decreases, the flow intensity increases very slightly. The effect of the parameter, a, on the apparent viscosity, μ, is given in Figure 9(b) where the viscosity increases with increasing parameter, a. Furthermore, Figure 9(a) and Figure 9(d) shows that the effect of the parameter, a, leads to a slight increase in the temperature and concentration difference in the wall.

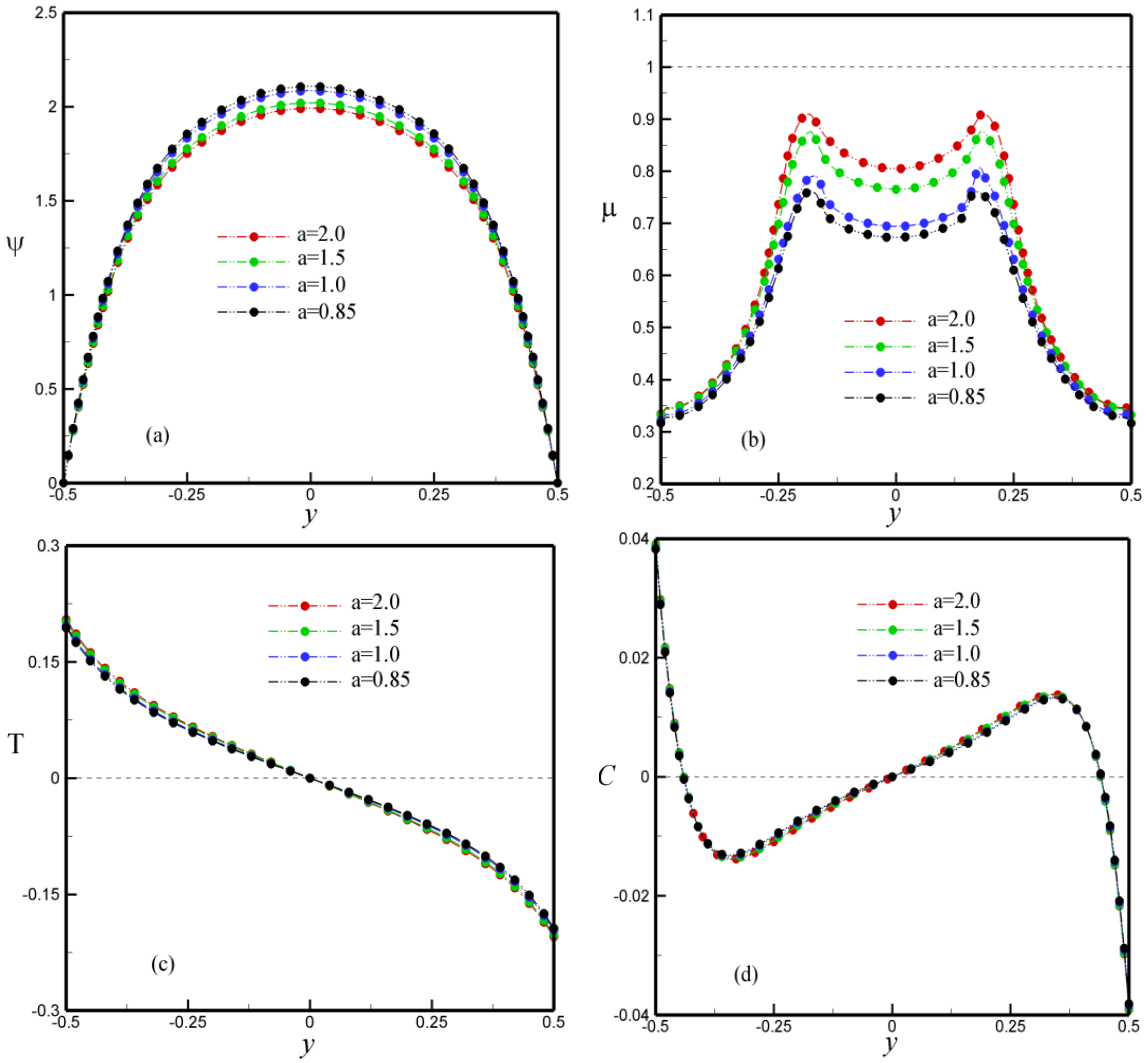

Fig. 9. Effect of parameter, a, on: (a) stream-function, ψ, (b) apparent viscosity, μ, (c) temperature, T, and (d) concentration, C, profiles for $R_T = 50$, $n = 0.6$, $s = 0.01$, $E = 0.2$, $Le = 10$, $N = -0.5$ and Φ=0°

Figure 10 clearly shows that the viscosity increases significantly with decreasing shear rate for different values of rheological parameters of Carreau-Yasuda. The viscosity is μ=1 when the fluid is Newtonian n=1 as shown in Figure 10(a). In contrast, in Figure 10(b), decreasing the parameter *E* induces an increase in viscosity μ=1 for *E=0*. This allows us to deduce that the apparent viscosity decreases with large values of *E*. We also observe that the apparent viscosity is favored by the increase of the parameter *s* when it takes a value of *s*=1. The viscosity is increased for the variation of the parameter a between 0.9 and 2.

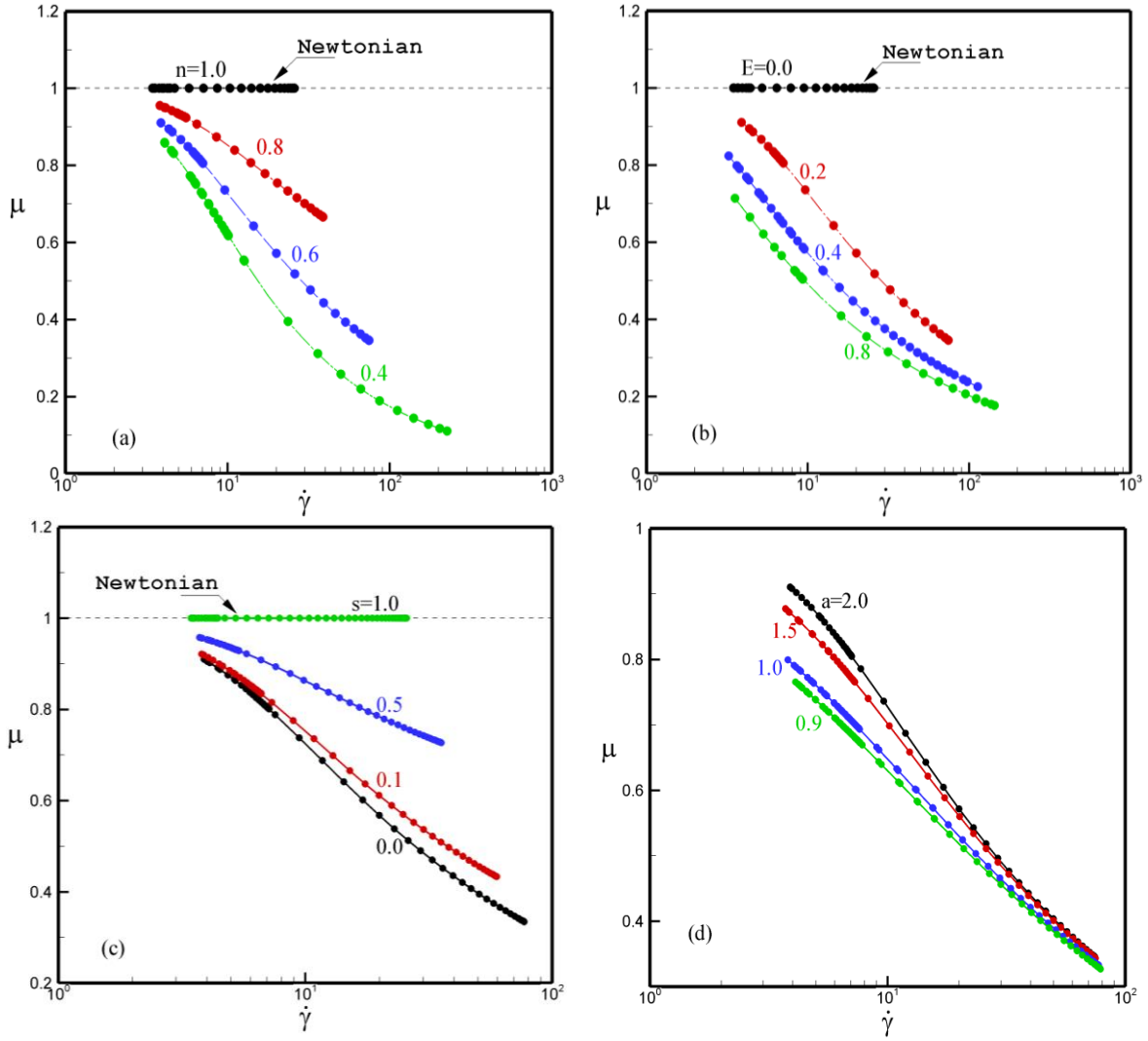

Fig. 10. Display the apparent viscosity, μ, with the shear rate, $\dot{\gamma}$, on: (a) effect of, n, (b) effect of time constant parameter, E, (c) effect of, s, and (d) effect of, a, for $Le = 10$, $R_T = 50$, $E = 0.2$, $a = 2$ and $s = 0.01$ and Φ=0°

Figure 11 shows the influence of the power-law index, *n*, on the flow intensity, apparent viscosity, Nusselt number and Sherwood number as a function of, R_T . The results clearly indicate that for given values of, *n*, there is a supercritical or subcritical Rayleigh number for a single-cell convection flow. Figure 11(a) shows that the convective flux improves with increasing, *n*. The same is true for the heat and mass transfer rates, which improves with increasing, *n*, (Figure 11(c) and Figure 11(d)). Decrease of the power-law index, *n*, leads to a decrease of the apparent viscosity whose main role is to reduce the viscous resistances on the one hand and to improve the convective flow on the other hand as shown in Figure 11(b). in the case of $\psi_0 = 0. Nu = Sh = 1$ and $\mu = 1$, the figure shows that the convection flux is supercritical below the critical value, the solution is purely conductive.

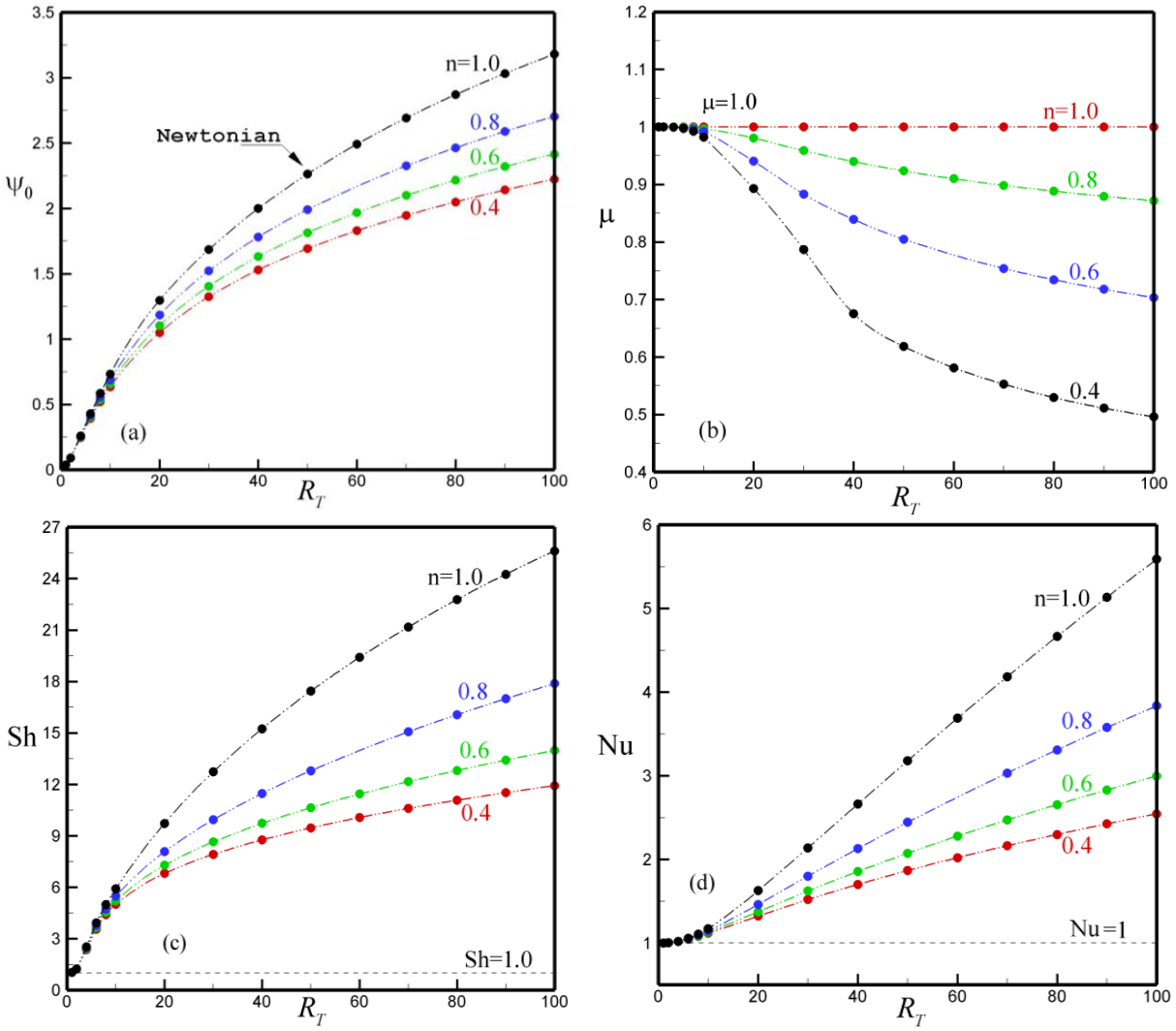

Fig. 11. Effect of, R_T , and power-law index, n, on: (a) stream function at the center of the cavity, ψ_0, (b) apparent viscosity, μ, (c) Sherwood number, Sh, and (d) Nusselt number, Nu, for $Le = 10$, $N = -0.5$, $n = 0.6$, $a = 2$, $s = 0.01$ and Φ=0°

Figure 12 shows the influence of parameter, E, on stream function, apparent viscosity, Sherwood number and Nusselt number versus power-law index, n. Figure 12(a) shows the flow function as a function of power-law index, n, such that the flow intensity increases with decreasing parameter, E, and increases with decreasing power-law index, n. The effect of parameter, E, on the apparent viscosity is shown in Figure 12(b) where the viscosity increases with decreasing parameter, E, from $E = 0.6$ (non-Newtonian fluids μ<1) to $E = 0$ (Newtonian fluids μ=1) and decreases with increasing power-law index (n). Furthermore, Figure 12(c) and Figure 12(d) show that a decrease in, E, leads to a decrease in the Sherwood number and Nusselt number, while when, n, decreases, the heat and mass exchange increases.

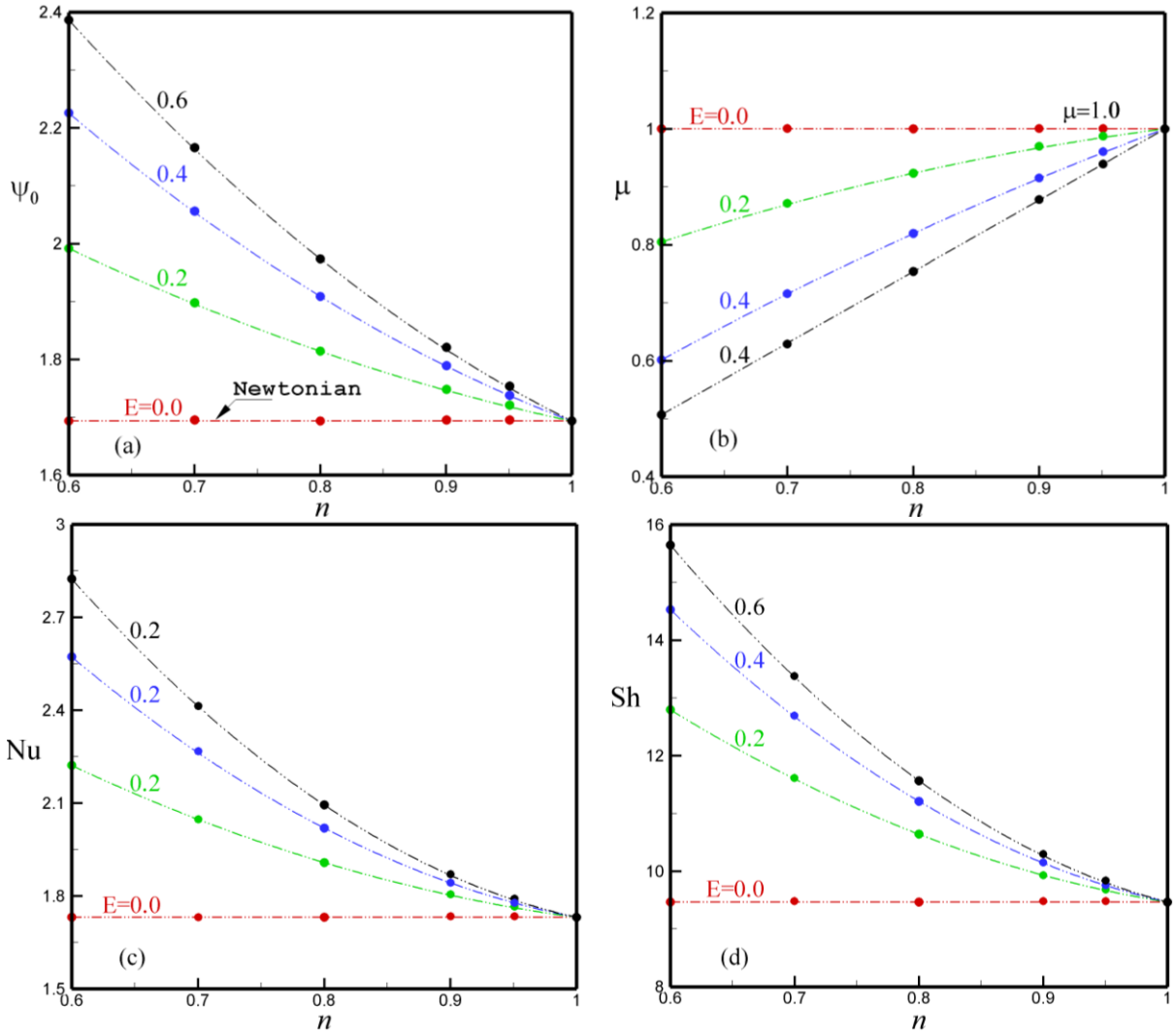

Fig. 12. Effect of parameter, E, and power-law index, n, on: (a) stream function at the center of the cavity, ψ_0, (b) apparent viscosity, μ, (c) Sherwood number, Sh, and (d) Nusselt number, Nu, for $R_T = 50$, $Le = 10$, $N = -0.5$, $a = 2$, $s = 0.01$ and Φ=0°

The result of the parameter, s, and, n, on the flow function, apparent viscosity, Sherwood number and Nusselt number is given in Figure 13. In Figure 13(a), the flow function decreases with increasing n. The viscosity increases with increasing n, reaching a maximum value at $n = 1$ (Newtonian fluids μ=1) as shown in Figure 13(b). Figure 13(c) and Figure 13(d) show that Sh and Nu decrease with increasing n, from 0.4 to 1, leading to an improvement in heat and mass exchange rates.

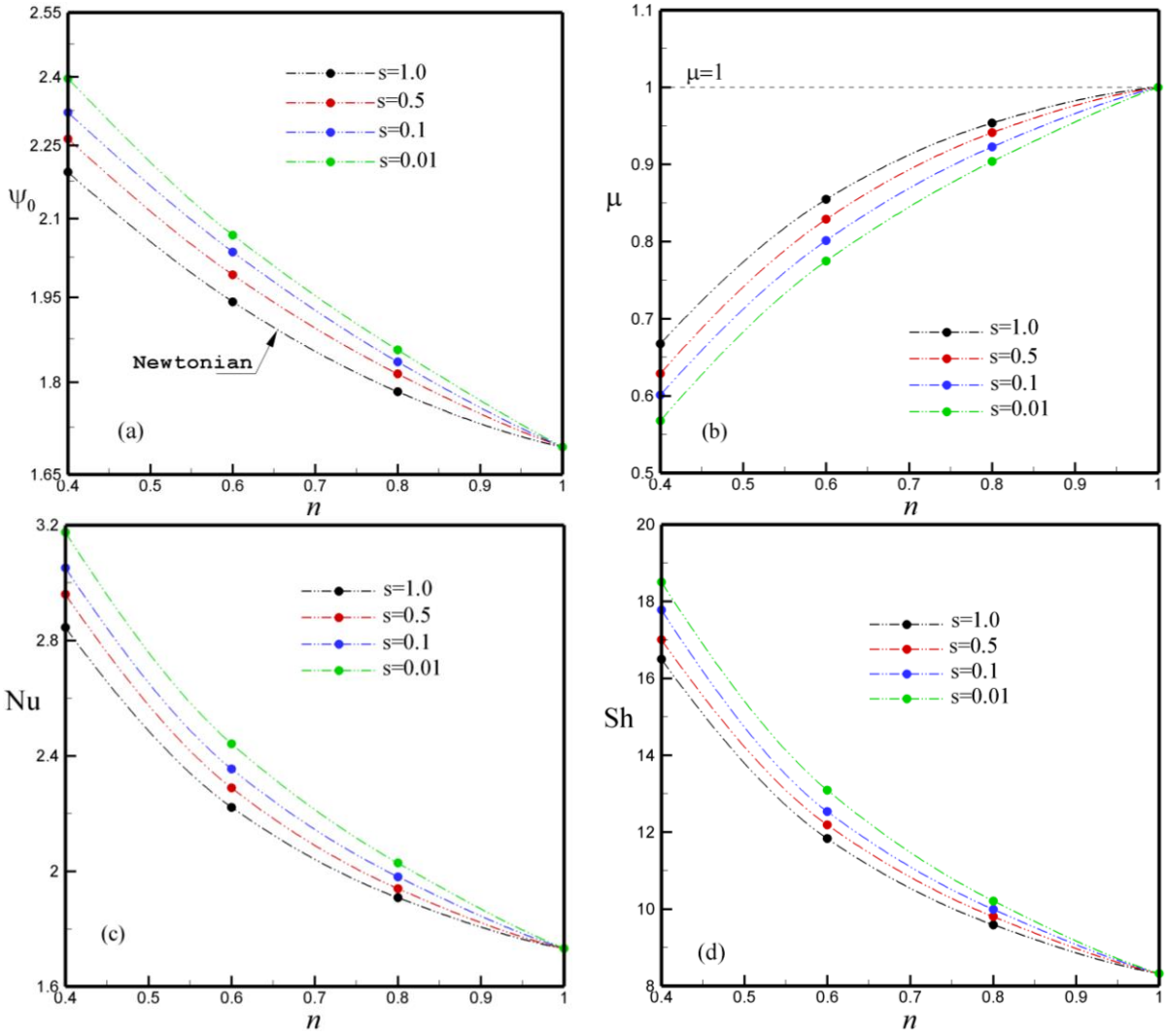

Fig. 13. Effect of the ratio of infinite-to zero-shear-rate viscosities, S, and power-law index, n, on: (a) stream function at the center of the cavity, ψ_0, (b) apparent viscosity, μ, (c) Sherwood number, Sh, and (d) Nusselt number, Nu, for $R_T = 50$, $Le = 10$, $N = -0.5$, $E = 0.2$, $a = 2$ and Φ=0°

Figure 14 illustrates the effects of parameter, a, on stream function, apparent viscosity, Sherwood number and Nusselt number as a function of power-law index, n. Figure 14(a) shows the changes in the flow function as a function of the power-law index, n, where the flow function increases with a decrease in both parameters, a. Figure 14(b) shows that an increase in the power index, n, and the parameter, a, of a lead to an increase in the apparent viscosity from μ<1 (non-Newtonian fluids) to $\mu = 1$ (Newtonian fluids). In addition, the influence of parameters, a, and, n, on the Sherwood number where Sherwood decreases slightly when the number, a, decreases and increases when the power-law index, n, decreases. The same explanation with the Nusselt number in Figure 14(d).

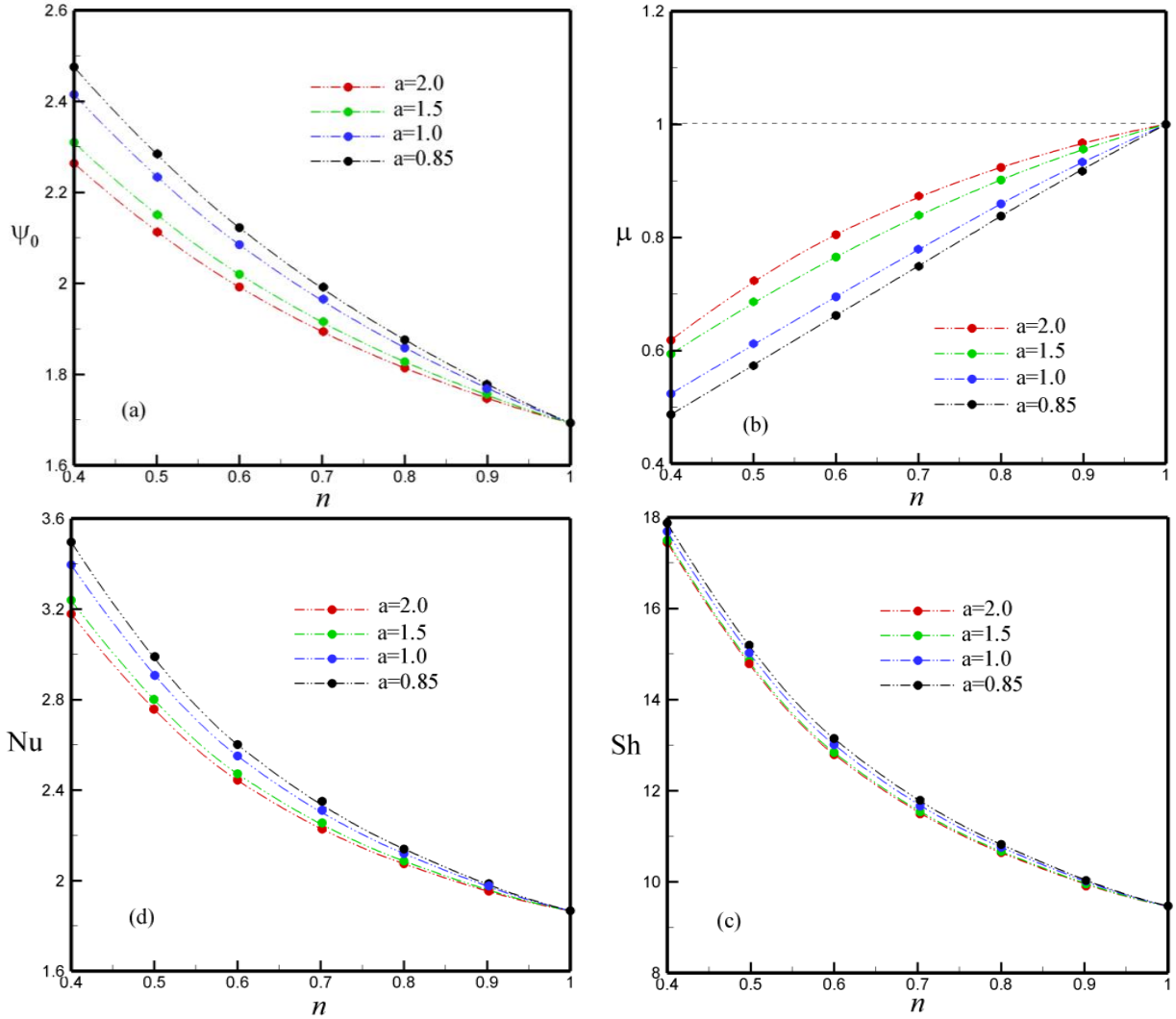

Fig. 14. Effect of parameter, a, and power-law index, n, on: (a) stream function at the center of the cavity, ψ_0, (b) apparent viscosity, μ, (c) Sherwood number, Sh, and (d) Nusselt number, Nu, for $R_T = 50$, $Le = 10$, $N = -0.5$, $E = 0.2$, $s = 0.01$ and Φ=0°

Figure 15 present the effects of, n, on the stream function, apparent viscosity, Sherwood and Nusselt number versus of buoyancy report, N. This covers the region where the flow becomes cooperative and dominated by solute effects (aid flow $N = 5$), the region where the flow is purely dominated by thermal effects (thermal flow $N = 0$), and the region where the forces are opposite but the flow by solute effects (reverse flow $N = -5$), i.e., (solutally dominated) the flow circulation is clockwise) ($\psi < 0$), see the streamlines in Figure 16(b). In the case $N = 0$, i.e., in the case where concentration effects are absent the convective motion is induced by the temperature gradients only which leads to a counter-clockwise circulation ($\psi > 0$), see the streamlines in Figure 16(a). On the other hand, the flow function increase with deceasing of the power-law index, n, as shown in Figure 15(a). In the case where N is greater than zero, the clockwise convective motion is said to be coincident, and the thermal and solute effects act in the same direction, and the flow of the current function is dominated by the buoyancy force. On the other hand, for N less than zero at $1.5 < N < 0$ when the thermal effect is dominant, the flow function is positive. In the same interval, the transition from the conductive to the convective regime when the number of, n, is deceased for $R_T = 50$ is lower than the number of supercritical, N_{cr}. Then, for large negative values, the solute effect is clear dominant and the flow becomes negative. Below the critical value, the solution is purely conductive

($\psi = 0$, $Nu = Sh = 1$) whatever the amplitude of the perturbation. The flow behavior depends strongly on the buoyancy rate, whether it is less than -1 or greater than -1, and it is found that the effect persists when the flow rate is zero. As n decreases from ($n = 1$ to $n = 0.4$) and, N, increases, we observe a slight difference in viscosity at μ = 1 (Newtonian fluids), and then decreases sharply to reach shear thinning values μ<1. Also, as n decreases and the buoyancy rate increases from -1 to 1, the number of Sh and Nu increases, confirming the improvement in thermal and mass exchange rates as shown in both Figure 16(c) and Figure 16(d).

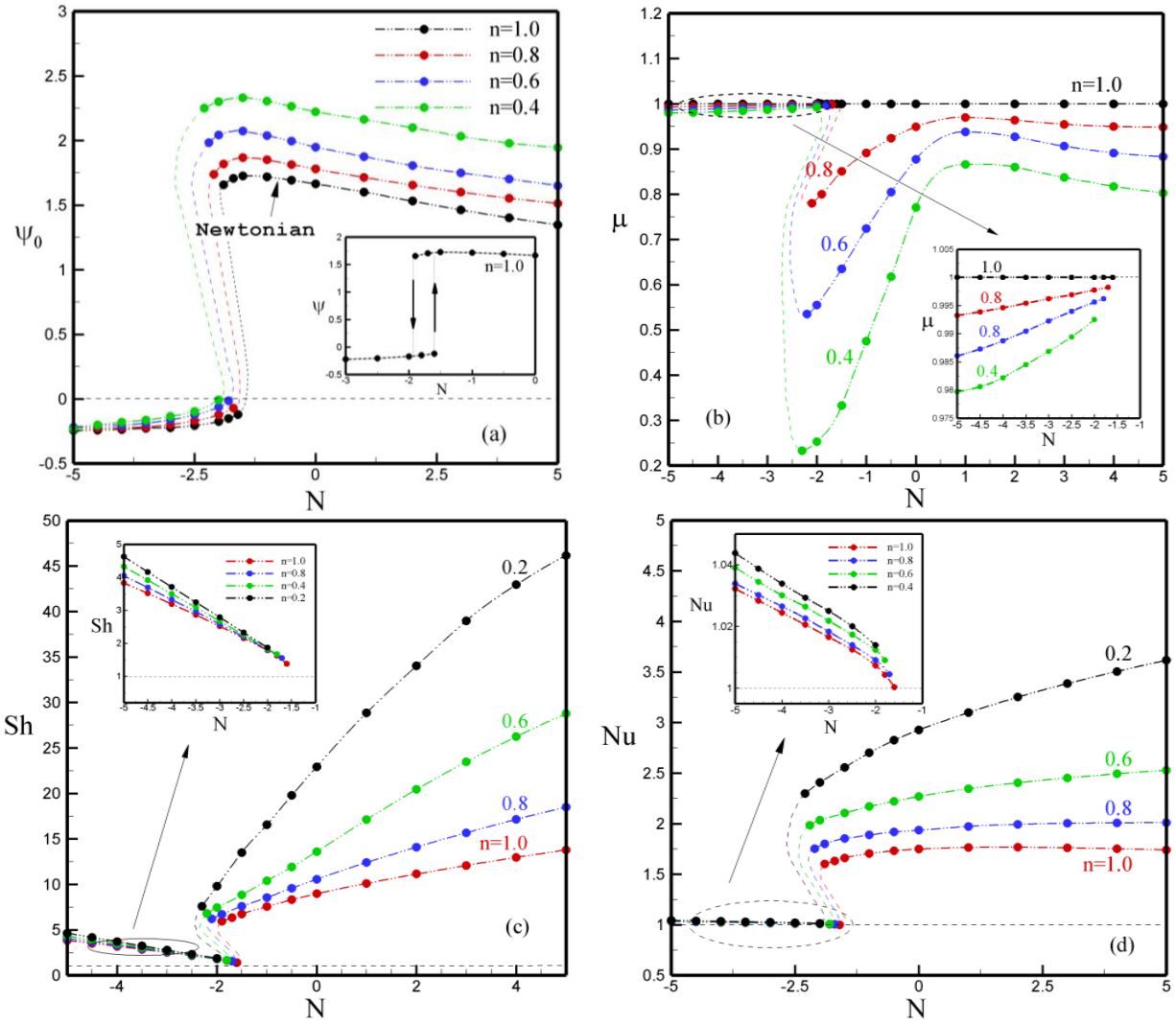

Fig. 15. Influence of buoyancy ratio, N, and, n, on: (a) stream function at the center of the cavity, ψ_0, (b) apparent viscosity, μ, (c) Sherwood number, Sh, and (d) Nusselt number, Nu, for $Le = 10$, $R_T = 50$, $E = 0.2$, $a = 2$, $s = 0.01$ and Φ=0°

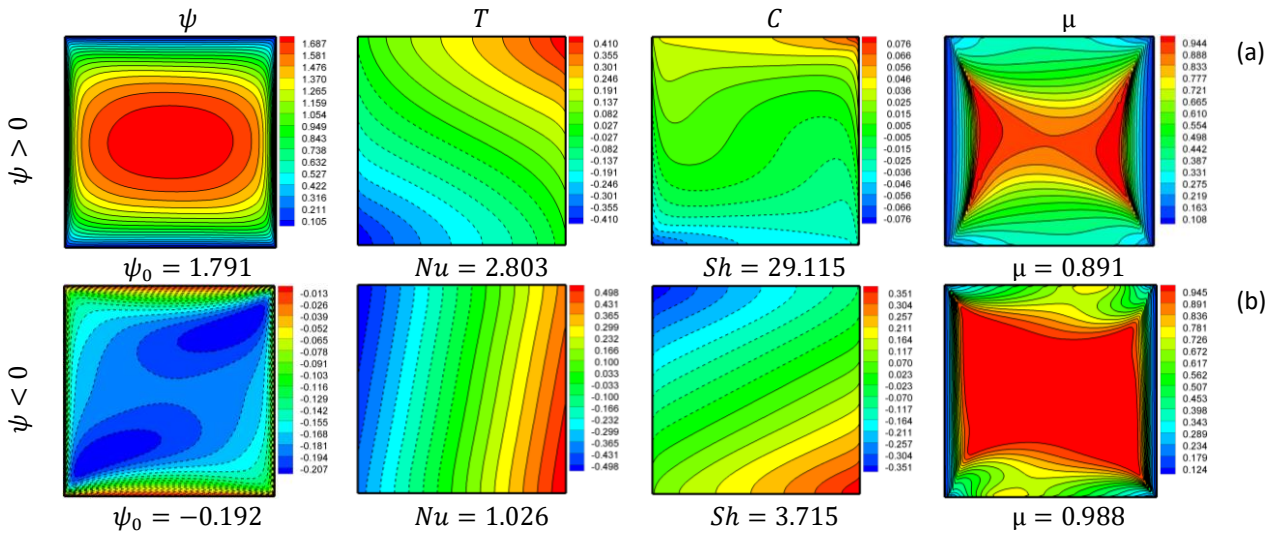

Fig. 16. Streamlines, isotherms, iso-concentrations and apparent viscosity from clockwise ($N > 0$) to counterclockwise ($N < 0$) for $R_T = 50$, $n = 0.6$, E = 0.2, S = 0.01, $a = 2$, $Le = 10$ and Φ=0°: (a) $N = 4$, (b) $N = -4$

The impact of Lewis number, Le, and, power-law index, n, on the stream function, apparent viscosity, Sherwood number and Nusselt numbers is presented in Figure 17. Figure 17(a) shows that the stream function increases significantly with the decrease of, n, to reach $\psi_0 = 2.263$ at the domain (Le=10^{-1} to Le=10^{1}), and then starts to decrease gradually to remain constant. Figure 17(b) shows the changes in apparent viscosity as a function of Le, for different amounts of n. As, n, increases and Le increases, the viscosity increases to $\mu = 1$ for $n = 1$ (Newtonian fluids). An increase in, Le, leads to an increase in Sh and Nu, and increases with decreasing power-law index. Furthermore, this confirms the improvement in mass and heat exchange, are plotted in Figure 6(c) and Figure 6(d).

Figure 18 display the effects of inclined angel, Φ, on stream function, apparent viscosity, Sherwood number and Nusselt number as a function of power-law index, n. The results show that a decrease in inclined angle leads to a significant increase in flow behavior as shown in Figure 18(a). Figure 18(b) shows a decrease in viscosity with an increase in, γ, and on the one hand, a decrease in the angle of inclination leads to a significant increase in, Sh, and, Nu, of Φ (30° to 90°) to reach their maximum value at $\Phi = 45°$. Furthermore, with a decrease in the power-law index, which led to an improvement in heat and mass, as show in Figure 18(c) and Figure 18(d).

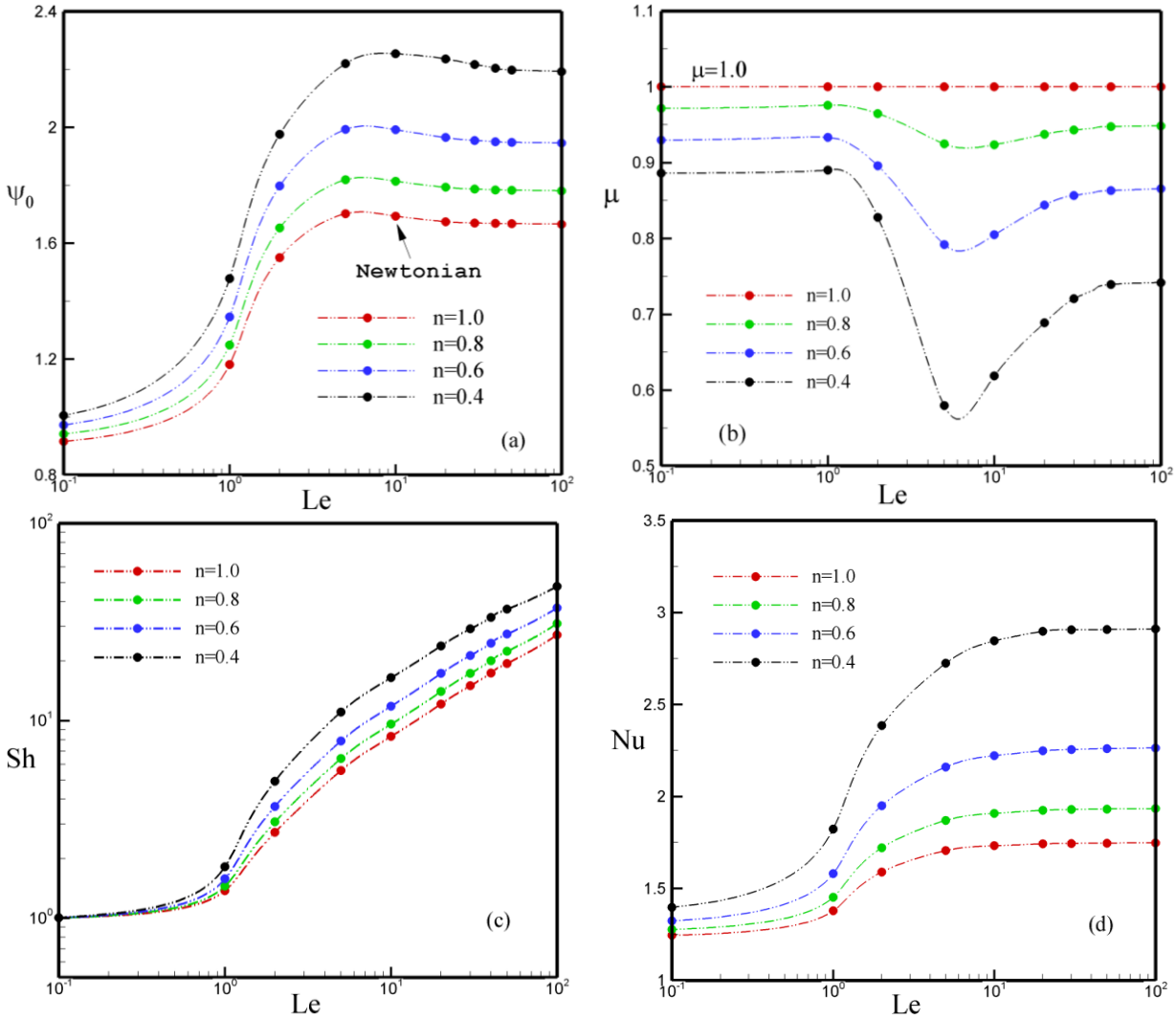

Fig. 17. Effect of, Le, and power-law index, n, on: (a) stream function, ψ_0, (b) apparent viscosity, μ, (c) Sherwood number, Sh, and (d) Nusselt number, Nu, for $R_T = 50$, $N = -0.5$, $a = 2$, $E = 0.2$, $s = 0.01$ and Φ=0°

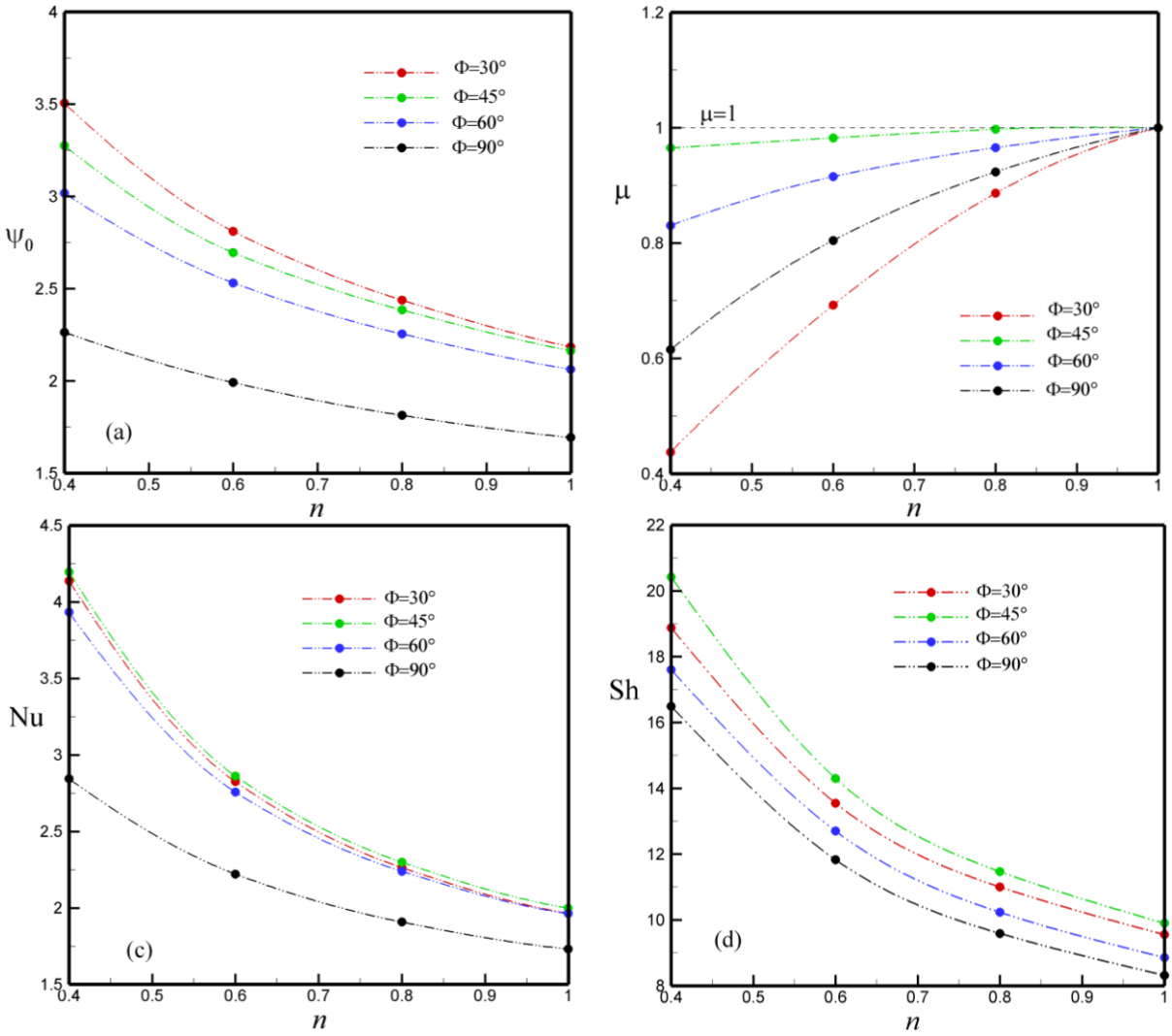

Fig. 18. Impact of inclined angel, Φ, and, n, on: (*a*) stream function at the center of the cavity, ψ_0, (*b*) apparent viscosity, μ, (*c*) Sherwood number, Sh, and (*d*) Nusselt number, Nu, for $Le = 10$, $Ra = 50$, $E = 0.2$, $a = 2$, $s = 0.01$ and $N = -0.5$

5. Conclusions

In this paper, we have presented the effect of rheological parameters on double-diffusive convection in a square porous medium saturated by non-Newtonian power-law fluids with yield stress. While the authors' walls were thought to be adiabatic and impermeable, the active walls were subjected to uniform heat and mass fluxes. The entire governing equation was used to arrive at the asymptotic numerical solution.

For some values of the governing parameters of the problem, the Rayleigh number R_T, and the four dimensionless parameters of the Carreau-Yasuda rheological model, namely: n, E, s, a and buoyancy ratio N, Lewis number Le, and inclination angle Φ, are obtained numerical results for the stream function, viscosity, temperature, and concentration.

As a result, the cavity's ability to transport heat is greatly impacted. The following is a summary of the investigation's principal conclusions

i. The temperature and concentration increase when the number of power-law indices, n, and E decreases. On the other hand, they increase when the parameters, s, decrease.

ii. It was discovered that for a particular set of Carreau-Yasuda parameters, the intensity of the mean viscosity reduces with a decrease in n and s as well as a decrease in E and a.
iii. The decrease in the Carreau-Yasuda parameters (n, E, s, a) and the increase in thermal Rayleigh have increased the flux density.
iv. In the total convection regime, the flow structure and the temperature and concentration fields are sensitive to a change in all parameters of Carreau-Yassuda model. Indeed, for a given thermal Rayleigh number, both the flow intensity and heat and mass transfers are favored when increasing (decreasing) the value of *E* and decreasing (increasing) the values of *s* and *n*.
v. For a given set of Carreau-Yasuda parameters, it was found that with an increase of R_T and a decrease of *n*, the mean viscosity strength decreases. Therefore, the heat transfer by convective heat transfer is enhanced with an increase in R_T and a decrease of *n*. For small values of the parameter, *n*, the flow can be oscillatory.
vi. Heat and mass transfer rates improved as the apparent viscosity decreased with the Rayleigh number and increased with the Lewis number.
vii. Increasing the Lewis number, *Le*, or decreasing the power-law index, *n*, increases the fluid circulation and heat and mass transfer rates. In addition, the Lewis number, Le, is found to play a role in favoring the contribution of the forced regime in the overall convection as it increases, especially when the power-law index, *n*, decreases.
viii. Increasing the buoyancy ratio, *N*, improves heat and mass transfer due to the prevailing buoyancy force. Moreover, the transition from conductive (for low values of the buoyancy force) to convective regime (higher buoyancy forces).
ix. The values of Nu and Sh increase as the angle of inclination decreases from 90° to 30°. Namely, the effect of the load is strongest at 45°.
x. The present study can be further extended to analyze the more complicated rheological behavior of other shear-thinning and shear-thickening fluid in a three-dimensional cavity model.

References

[1] Combarnous, M. A., and S. A. Bories. "Hydrothermal convection in saturated porous media." In *Advances in Hydroscience*, vol. 10, pp. 231-307. Elsevier, 1975. https://doi.org/10.1016/B978-0-12-021810-3.50008-4
[2] Nield, Donald A., and Adrian Bejan. *Convection in porous media*. New York: Springer, 1992. https://doi.org/10.1007/978-1-4757-2175-1
[3] Xin, Shihe, Patrick Le Quéré, and Laurette S. Tuckerman. "Bifurcation analysis of double-diffusive convection with opposing horizontal thermal and solutal gradients." *Physics of Fluids* 10, no. 4 (1998): 850-858. https://doi.org/10.1063/1.869608
[4] Çıbık, Aytekin, and Songül Kaya. "Finite element analysis of a projection-based stabilization method for the Darcy-Brinkman equations in double-diffusive convection." *Applied Numerical Mathematics* 64 (2013): 35-49. https://doi.org/10.1016/j.apnum.2012.06.034
[5] Khan, Ansab Azam, Khairy Zaimi, Suliadi Firdaus Sufahani, and Mohammad Ferdows. "MHD flow and heat transfer of double stratified micropolar fluid over a vertical permeable shrinking/stretching sheet with chemical reaction and heat source." *Journal of Advanced Research in Applied Sciences and Engineering Technology* 21, no. 1 (2020): 1-14. https://doi.org/10.37934/araset.21.1.114
[6] Wang, Jin, Mo Yang, and Yuwen Zhang. "Onset of double-diffusive convection in horizontal cavity with Soret and Dufour effects." *International Journal of Heat and Mass Transfer* 78 (2014): 1023-1031. https://doi.org/10.1016/j.ijheatmasstransfer.2014.07.064
[7] Chen, Han-Taw, and Cha'o-Kuang Chen. "Natural convection of a non-Newtonian fluid about a horizontal cylinder and a sphere in a porous medium." *International Communications in Heat and Mass Transfer* 15, no. 5 (1988): 605-614. https://doi.org/10.1016/0735-1933(88)90051-6

[8] Yang, Yue-Tzu, and Sae-Jan Wang. "Free convection heat transfer of non-Newtonian fluids over axisymmetric and two-dimensional bodies of arbitrary shape embedded in a fluid-saturated porous medium." *International Journal of Heat and Mass Transfer* 39, no. 1 (1996): 203-210. https://doi.org/10.1016/S0017-9310(96)85016-2

[9] Mahrous, Samar A., Nor Azwadi Che Sidik, and Khalid M. Saqr. "Newtonian and non-Newtonian CFD models of intracranial aneurysm: a review." *CFD Letters* 12, no. 1 (2020): 62-86.

[10] Pascal, H. "Rheological behaviour effect of non-newtonian fluids on steady and unsteady flow through a porous medium." *International Journal for Numerical and Analytical Methods in Geomechanics* 7, no. 3 (1983): 289-303. https://doi.org/10.1002/nag.1610070303

[11] Pascal, H. "Rheological effects of non-Newtonian behavior of displacing fluids on stability of a moving interface in radial oil displacement mechanism in porous media." *International Journal of Engineering Science* 24, no. 9 (1986): 1465-1476. https://doi.org/10.1016/0020-7225(86)90157-6

[12] Taunton, J. W., E. N. Lightfoot, and Theodore Green. "Thermohaline instability and salt fingers in a porous medium." *The Physics of Fluids* 15, no. 5 (1972): 748-753. https://doi.org/10.1063/1.1693979

[13] Jumah, Rami Y., and Arun S. Mujumdar. "Natural convection heat and mass transfer from a vertical flat plate with variable wall temperature and concentration to power-law fluids with yield stress in a porous medium." *Chemical Engineering Communications* 185, no. 1 (2001): 165-182. https://doi.org/10.1080/00986440108912861

[14] Al-Azawy, Mohammed Ghalib, Saleem Khalefa Kadhim, and Azzam Sabah Hameed. "Newtonian and non-newtonian blood rheology inside a model of stenosis." *CFD Letters* 12, no. 11 (2020): 27-36. https://doi.org/10.37934/cfdl.12.11.2736

[15] Unuh, M. H., P. Muhamad, H. M. Y. Norfazrina, M. A. Ismail, and Z. Tanasta. "Study of Magnetic Flux and Shear Stress of OEM Damper featuring MR Fluid." *Journal of Advanced Research in Applied Mechanics* 41, no. 1 (2018): 9-15.

[16] Wang, Shih-Chieh, Cha'o-Kuang Chen, and Yue-Tzu Yang. "Natural convection of non-Newtonian fluids through permeable axisymmetric and two-dimensional bodies in a porous medium." *International Journal of Heat and Mass Transfer* 45, no. 2 (2002): 393-408. https://doi.org/10.1016/S0017-9310(01)00123-5

[17] Jecl, Renata, and Leopold Škerget. "Boundary element method for natural convection in non-Newtonian fluid saturated square porous cavity." *Engineering Analysis with Boundary Elements* 27, no. 10 (2003): 963-975. https://doi.org/10.1016/S0955-7997(03)00077-8

[18] Lamsaadi, M., M. Naimi, and M. Hasnaoui. "Natural convection of non-Newtonian power law fluids in a shallow horizontal rectangular cavity uniformly heated from below." *Heat and Mass Transfer* 41, no. 3 (2005): 239-249. https://doi.org/10.1007/s00231-004-0530-8

[19] Bahloul, Ali. "Boundary layer and stability analysis of natural convection in a porous cavity." *International Journal of Thermal Sciences* 45, no. 7 (2006): 635-642. https://doi.org/10.1016/j.ijthermalsci.2005.10.003

[20] Cheng, Ching-Yang. "Natural convection heat and mass transfer of non-Newtonian power law fluids with yield stress in porous media from a vertical plate with variable wall heat and mass fluxes." *International Communications in Heat and Mass Transfer* 33, no. 9 (2006): 1156-1164. https://doi.org/10.1016/j.icheatmasstransfer.2006.06.006

[21] Hadim, H. "Non-Darcy natural convection of a non-Newtonian fluid in a porous cavity." *International Communications in Heat and Mass Transfer* 33, no. 10 (2006): 1179-1189. https://doi.org/10.1016/j.icheatmasstransfer.2006.08.004

[22] Lin, Changhao, and L. E. Payne. "Continuous dependence on the Soret coefficient for double diffusive convection in Darcy flow." *Journal of Mathematical Analysis and Applications* 342, no. 1 (2008): 311-325. https://doi.org/10.1016/j.jmaa.2007.11.036

[23] Rebhi, Redha, Noureddine Hadidi, Mahmoud Mamou, Khaled Khechiba, and R. Bennacer. "The onset of unsteady double-diffusive convection in a vertical porous cavity under a magnetic field and submitted to uniform fluxes of heat and mass." *Special Topics & Reviews in Porous Media: An International Journal* 11, no. 3 (2020): 259-285. https://doi.org/10.1615/SpecialTopicsRevPorousMedia.2020030120

[24] Rebhi, Redha, Noureddine Hadidi, and Rachid Bennacer. "Non-Darcian effect on double-diffusive natural convection inside aninclined square Dupuit-Darcy porous cavity under a magnetic field." *Thermal Science* 25, no. 1 Part A (2021): 121-132. https://doi.org/10.2298/TSCI190117271R

[25] Chamkha, Ali J. "Heat and mass transfer of a non-Newtonian fluid flow over a permeable wedge in porous media with variable wall temperature and concentration and heat source or sink." *WSEAS Transactions on Heat and Mass Transfer* 5, no. 1 (2010): 11-20.

[26] Kefayati, GH. R. "Simulation of double diffusive natural convection and entropy generation of power-law fluids in an inclined porous cavity with Soret and Dufour effects (Part I: Study of fluid flow, heat and mass transfer)." *International Journal of Heat and Mass Transfer* 94 (2016): 539-581. https://doi.org/10.1016/j.ijheatmasstransfer.2015.11.044

[27] Kefayati, GH R. "Simulation of double diffusive natural convection and entropy generation of power-law fluids in an inclined porous cavity with Soret and Dufour effects (Part II: Entropy generation)." *International Journal of Heat and Mass Transfer* 94 (2016): 582-624. https://doi.org/10.1016/j.ijheatmasstransfer.2015.11.043
[28] Khechiba, Khaled, Mahmoud Mamou, Madjid Hachemi, Nassim Delenda, and Redha Rebhi. "Effect of Carreau-Yasuda rheological parameters on subcritical Lapwood convection in horizontal porous cavity saturated by shear-thinning fluid." *Physics of Fluids* 29, no. 6 (2017): 063101. https://doi.org/10.1063/1.4986794
[29] Zhu, Q. Y., Y. J. Zhuang, and H. Z. Yu. "Three-dimensional numerical investigation on thermosolutal convection of power-law fluids in anisotropic porous media." *International Journal of Heat and Mass Transfer* 104 (2017): 897-917. https://doi.org/10.1016/j.ijheatmasstransfer.2016.09.018
[30] Wahid, Nur Syahirah, Mohd Ezad Hafidz Hafidzuddin, Norihan Md Arifin, Mustafa Turkyilmazoglu, and Nor Aliza Abd Rahmin. "Magnetohydrodynamic (MHD) Slip Darcy Flow of Viscoelastic Fluid Over A Stretching Sheet and Heat Transfer with Thermal Radiation and Viscous Dissipation." *CFD Letters* 12, no. 1 (2020): 1-12.
[31] Parvin, Shahanaz, Siti Suzilliana Putri Mohamed Isa, Norihan Md Arifin, and Fadzilah Md Ali. "The Magnetohydrodynamics Casson Fluid Flow, Heat and Mass Transfer Due to the Presence of Assisting Flow and Buoyancy Ratio Parameters." *CFD Letters* 12, no. 8 (2020): 64-75. https://doi.org/10.37934/cfdl.12.8.6475
[32] Rebhi, Redha, Mahmoud Mamou, Patrick Vasseur, and Mounir Alliche. "Form drag effect on the onset of non-linear convection and Hopf bifurcation in binary fluid saturating a tall porous cavity." *International Journal of Heat and Mass Transfer* 100 (2016): 178-190. https://doi.org/10.1016/j.ijheatmasstransfer.2016.04.060
[33] Rebhi, Redha, Mahmoud Mamou, and Patrick Vasseur. "Bistability and hysteresis induced by form drag in nonlinear subcritical and supercritical double-diffusive Lapwood convection in shallow porous enclosures." *Journal of Fluid Mechanics* 812 (2017): 463-500. https://doi.org/10.1017/jfm.2016.787
[34] Khan, M. Ijaz, Faris Alzahrani, Aatef Hobiny, and Zulfiqar Ali. "Estimation of entropy optimization in Darcy-Forchheimer flow of Carreau-Yasuda fluid (non-Newtonian) with first order velocity slip." *Alexandria Engineering Journal* 59, no. 5 (2020): 3953-3962. https://doi.org/10.1016/j.aej.2020.06.057
[35] Mutschler, Dimitri, and Abdelkader Mojtabi. "Theoretical and numerical analysis of Soret-driven convection in a horizontal porous layer saturated by an n-component mixture: Application to ternary hydrocarbon mixture tetralin, isobutyl benzene, n-dodecane with mass fractions 0.8-0.1-0.1." *International Journal of Heat and Mass Transfer* 162 (2020): 120339. https://doi.org/10.1016/j.ijheatmasstransfer.2020.120339
[36] Ali, Amjad, Hamayun Farooq, Zaheer Abbas, Zainab Bukhari, and Attia Fatima. "Impact of Lorentz force on the pulsatile flow of a non-Newtonian Casson fluid in a constricted channel using Darcy's law: a numerical study." *Scientific Reports* 10, no. 1 (2020): 1-15. https://doi.org/10.1038/s41598-020-67685-0
[37] Ghiasi, Emran Khoshrouye, and Reza Saleh. "Analytical and numerical solutions to the 2D Sakiadis flow of Casson fluid with cross diffusion, inclined magnetic force, viscous dissipation and thermal radiation based on Buongiorno's mathematical model." *CFD Letters* 11, no. 1 (2019): 40-54.
[38] Wang, Fuzhang, Muhammad Imran Asjad, Saif Ur Rehman, Bagh Ali, Sajjad Hussain, Tuan Nguyen Gia, and Taseer Muhammad. "MHD Williamson Nanofluid Flow over a Slender Elastic Sheet of Irregular Thickness in the Presence of Bioconvection." *Nanomaterials* 11, no. 9 (2021): 2297. https://doi.org/10.3390/nano11092297
[39] Khdher, Abdolbaqi Mohammed, Nor Azwadi Che Sidik, Siti Nurul Akmal Yusof, and M'hamed Beriache. "Heat Transfer Enhancement in Straight Channel with Nanofluid In Fully Developed Turbulent Flow." *Journal of Advanced Research in Applied Mechanics* 63, no. 1 (2019): 1-15.
[40] Yusof, Nur Syamila, Siti Khuzaimah Soid, Mohd Rijal Illias, Ahmad Sukri Abd Aziz, and Nor Ain Azeany Mohd Nasir. "Radiative Boundary Layer Flow of Casson Fluid Over an Exponentially Permeable Slippery Riga Plate with Viscous Dissipation." *Journal of Advanced Research in Applied Sciences and Engineering Technology* 21, no. 1 (2020): 41-51. https://doi.org/10.37934/araset.21.1.4151
[41] Khan, Shahid Ali, Chika Eze, Kwun Ting Lau, Bagh Ali, Shakeel Ahmad, Song Ni, and Jiyun Zhao. "Study on the novel suppression of heat transfer deterioration of supercritical water flowing in vertical tube through the suspension of alumina nanoparticles." *International Communications in Heat and Mass Transfer* 132 (2022): 105893. https://doi.org/10.1016/j.icheatmasstransfer.2022.105893
[42] Habib, Danial, Nadeem Salamat, Muhammad Ahsan, Sohaib Abdal, Imran Siddique, and Bagh Ali. "Significance of bioconvection and mass transpiration for MHD micropolar Maxwell nanofluid flow over an extending sheet." *Waves in Random and Complex Media* (2022): 1-15. https://doi.org/10.1080/17455030.2022.2088892
[43] Awan, Aziz Ullah, N. Ameer Ahammad, Sonia Majeed, Fehmi Gamaoun, and Bagh Ali. "Significance of hybrid nanoparticles, Lorentz and Coriolis forces on the dynamics of water based flow." *International Communications in Heat and Mass Transfer* 135 (2022): 106084. https://doi.org/10.1016/j.icheatmasstransfer.2022.106084
[44] Rebhi, Redha, Mahmoud Mamou, and Noureddine Hadidi. "Bistability bifurcation phenomenon induced by non-Newtonian fluids rheology and thermosolutal convection in Rayleigh-Bénard convection." *Physics of Fluids* 33, no. 7 (2021): 073104. https://doi.org/10.1063/5.0051058

[45] Lounis, Selma, Redha Rebhi, Noureddine Hadidi, Giulio Lorenzini, Younes Menni, Houari Ameur, and Nor Azwadi Che Sidik. "Thermo-Solutal Convection of Carreau-Yasuda Non-Newtonian Fluids in Inclined Square Cavities Under Dufour and Soret Impacts." *CFD Letters* 14, no. 3 (2022): 96-118. https://doi.org/10.37934/cfdl.14.3.96118
[46] Yasuda, K. Y., R. C. Armstrong, and R. E. Cohen. "Shear flow properties of concentrated solutions of linear and star branched polystyrenes." *Rheologica Acta* 20, no. 2 (1981): 163-178. https://doi.org/10.1007/BF01513059
[47] Bird, R. Byron, Robert C. Armstrong, and Ole Hassager. *Dynamic of polymeric liquids*. John Wiley and Sons, 1978.
[48] Escudier, M. P., I. W. Gouldson, A. S. Pereira, F. T. Pinho, and R. J. Poole. "On the reproducibility of the rheology of shear-thinning liquids." *Journal of Non-Newtonian Fluid Mechanics* 97, no. 2-3 (2001): 99-124. https://doi.org/10.1016/S0377-0257(00)00178-6
[49] Gray, Donald D., and Aldo Giorgini. "The validity of the Boussinesq approximation for liquids and gases." *International Journal of Heat and Mass Transfer* 19, no. 5 (1976): 545-551. https://doi.org/10.1016/0017-9310(76)90168-X
[50] Benhadji, Khalid Brahim. "Convection thermo-solutale au sein d'une cavité poreuse saturée par un fluide non newtonien binaire." *Master diss., École Polytechnique de Montréal* (2001).
[51] Mamou, M., and P. Vasseur. "Thermosolutal bifurcation phenomena in porous enclosures subject to vertical temperature and concentration gradients." *Journal of Fluid Mechanics* 395 (1999): 61-87. https://doi.org/10.1017/S0022112099005753